Response to the comments of Anonymous Reviewer #1

We would like to thank the reviewers for their constructive and helpful comments! We give our response as:

Reviewer comment – Authors' response where needed – Changes to manuscript.

Title: Consider changing the title. I'm not sure if explaining is the right word. The study leaves many questions open, so maybe studying would be more appropriate word.
We change the title to "Investigating drivers of interdecadal salinity changes in the Baltic Sea in a 1850-2008 hindcast simulation"

Introduction: In the introduction, you could also introduce some literature related to the drivers of the salinity variation you are discussing later on; e.g. NAO, AMO and how their effects to the Baltic Sea dynamics have been studied earlier. Please avoid introducing your results in the introduction (e.g. line 60)
We include more references to existing research and remove the results from the introduction.

Material and Methods: In the dataset-section, consider using subtitles. It is easier to find, what you are looking for, when one is later on returning to this section to check what was said here.
We structure section 2.1 by introducing the following headings: "ICES T and S observations", "HIRESAFF v2 atmospheric reconstruction", "River runoff", "Baltic Inflow reconstruction" and "Climate indices".

Model validation: Consider putting surface and bottom salinities to different figures or use larger image size. With the current size, scales and colours it is difficult to see the differences between the measurements and the model.
We find that yet another set of seven figures would be too many, since the manuscript is already packed with figures.
We will ask the typesetter to skip the width limitation which makes the figure substantially smaller than the two-column text. We will also use a broken y-axis at strongly stratified stations to increase the vertical scale of the temporal variations.

Results of the wavelet analysis: The amount of stations and parameters studied is bit exhausting and it is not easy to form a consistent overview of the different effects and time scales. Would it be possible to summarize the main findings in a table?
Thank you for this excellent suggestion!
We add a table summarizing the main findings of the wavelet analysis method.

Discussion: In discussion of the things affecting the model accuracy in the beginning of the model period, you could also include the accuracy of the atmospheric forcing. I do not know the details of the forcing dataset used here, but typically the amount of data assimilated in the models increases the nearer we come to present and therefore typically also the accuracy improves. This would also affect the accuracy of the ocean model as the simulation of the MBI's are sensitive to the accuracy of the atmospheric forcing.
We will add this point to the discussion.

Drivers and variation: I would like to see more discussion on the combined effect of the different drivers. Although it is now easy to study this, you could at least discuss the possible joint effects of the different drivers, as they are not independent from one another.

We see your point. However, we cannot go into detail in this study since obviously numerous interactions can exist.

We mention the possibility of non-linear interactions between different drivers in the outlook section.

Conclusions and outlook: I would avoid using the world realistic, when talking about hindcast simulation. Maybe some other term related to quality?

We omit “realistic”.

Response to the comments of Anonymous Reviewer #2

We would like to thank the reviewers for their constructive and helpful comments! We give our response as:

Reviewer comment – Authors' response where needed – Changes to manuscript.

I find the quantification of the effects of river runoff and inflows on the salinity variation in the Baltic are of interest to the scientific community. The main benefit of the study could be to present actual numbers. The authors appear to refrain so in both the abstract and the conclusions. Oddly they present numbers in the Outlook (pg. 28 ln.490). I wonder why.

The wavelet coherence method we apply does not allow a quantification of the relative importance, so we cannot give actual numbers. We do give numbers for the second method, the direct dilution effect.

Sensitivity model simulations are necessary for the quantification of the drivers' influence, which we discuss in the outlook section. The given numbers represent guesses for the outcome of the presently running sensitivity experiments and are based on the assumption that our model results agree with those of Meier and Kauker (2003b), as we wrote: "This suggests that if the models agree, both direct and indirect effect of river runoff could explain about 50% of the salinity changes."

We add a sentence: "We will do so in future sensitivity runs."

In addition, I am worried by the model results summarized in Table 1: The Baltic is essentially a number of basins interconnected by shallow sills. Saline inflows (which are found by the authors to be a major process setting salinity variability) enter via the Danish Straits, travel at depth via the Arkona Basin, the Bornholm Basin into the Baltic Proper. In the Bornholm Basin simulated deep salinities are anticorrelated to observations (Station BY5 in Tab. 1). This suggests that simulated deep waters flowing out of the Bornholm Basin into the Baltic proper have the wrong salinities. This, in turn, suggests a deficient representation of inflows in the model. The fact that the fit to observations increases further downstream in the Baltic Proper (Station BY15in Tab. 1) even though it is so bad upstream suggests: (1) inflows do not dominate deep salinities in the Baltic, or (2) two deficient processes (deficient inflow and maybe mixing) add up to a reasonable result (i.e. fit to observed salinities).

For inflows into the Eastern Gotland Basin (Station BY15), not only the salinities at BY5 but also the volumes pushed across Slupsk Furrow are important. It is hard to tell because of lacking observations, but we suppose that these volumes are more important and better captured by our model.

Maybe Tab. 1 is wrong? It is hard to tell from Figure 5.

We have checked Table 1 and found it correct. The bad fit at BY5 may also be a result of the incompleteness of the observation data, which implies that the strong interannual variability in the salinities is misinterpreted as decadal variations when too few years of a decade contribute to the mean.

I recommend to discuss the evolution along the typical path of a saline inflow event from initially worsening (Station BY2 to BY5) and subsequently increasing (Station BY5 to BY15) fit to observed deep salinities.

We add a discussion in the online supplement.

Minor comments: Abstract: Would be nice if some numerical metric could be included such as e.g.: Our model explains xx% of the variance inherent to available observations. We find that xx% of the variance in our model is associated to process A and yy% to process B.

This is not possible for the wavelet decomposition method.

We add the explained variances at station BY15 and the number of 27% for the direct dilution effect to the abstract.

Maybe add a sentence on why interdecadal salinity changes in the Baltic are of interest.
We explained the importance of species' adaptation to brackish salinities for the Baltic Sea ecosystem. We see this as the major reason why salinity changes are important to understand.

We will add a sentence to the abstract which indicates this motivation for our study.

pg. 1 ln. 12 "spurious" replace with accidental, coincidentally ...
We will replace with coincidental.

pg. 1 ln. 10 "As a consequence ..." Please explain why this is a consequence. It is not obvious.
The salt budget of the bottom water requires that salt import due to inflows will be compensated for by salt export due to upward diffusion. We will not explain it in the abstract.

pg. 2 ln.48: "Still it is questionable ...": rephrase
Rephrased to "This does, however, not necessarily mean that the salinity variations are caused by a direct dilution effect."

pg. 3 ln. 57: We demonstrate ... allows fora new perspective": Sounds very elegant but is pretty meaningless. Please be morespecific here.
We replace "allows new perspectives on the influence of runoff on salinity" by "suggests a limited influence of runoff on salinity".

pg. 3 ln. 64-67: Remains unclear if you do that in the paper. If it is only meant to justify what you are doing in the paper then maybe put it more towards the beginning of the introduction.
We move this paragraph between lines 33 and 34.

pg. 6 Model simulation: someplace earlier in the text you have been talking about two different models (a 3d and a box model) so I would have expected: "Model simulations" or at least an introductory sentence concerning the number of different models used in the study.
We will include an introductory sentence as suggested.

pg. 8 ln. 182: I like the list. Maybe add some more information as to where the data originates from (such as e.g. to item2 3 and 4).
We will put the source in parentheses after each bullet point.

pg. 10 "3 Model validation": one wonders which model; please specify
Will be changed to "Numerical model validation".

Fig. 5.: By putting both surface and bottom salinities into one plot model-data misfits are dwarfed. This appears dodgy to me.
We do not want to introduce even more figures. The figure appears small as it is limited to a fraction of the page width.
We will ask the typesetter to print the figure larger. We will also use a broken y-axis where surface and bottom salinities deviate too much.

pg. 11 ln. 252: I do not understand this reasoning. Please explain more comprehensively.
We will (a) give a formula how we calculate explained variance and (b) refer to a discussion of this issue in the online supplement.

pg. 12 Table 1: the concept of negative explained variance is somewhat odd.
Explained variance is never negative in linear regression, where it is given as R^2. Our model is, however, not a linear one, so the variance in the residuals can be larger than that in the original data, resulting in negative explained variance.

Response to Short Comment 1 by Katharina Höflich

We would like to thank Mrs Höflich for her constructive and helpful comments! We give our response as:

Short comment – Authors' response where needed – Changes to manuscript.

5. Are the results sufficient to support the interpretations and conclusions?
very likely; however, the structure of the paper is not very easily grasped; therefore, it is difficult to decide if everything is consistent and conclusive
Indeed the structure of our paper deviates from the standard because we use two techniques (Wavelet coherence / box model for estimation of direct runoff effect) and do not want to skip any of them. If we kept to the classical structure (methods, results, discussion), this would mean alternating between the two (methods wavelet – methods runoff effect – results wavelet – results runoff effect – discussion wavelet – discussion runoff effect) and this might be even harder to follow for the reader. So, we prefer to keep the existing structure.

6. Is the description of experiments and calculations sufficiently complete and precise to allow their reproduction by fellow scientists?
not in every aspect, e.g. please provide more details on the significance analysis of the signals appearing in the wavelet decompositon/coherence analysis; have you considered the papers by Douglas Maraun (e.g. 10.5194/npg-11-505-2004) here?
Thank you for pointing at this reference here. Indeed we follow the suggestion giving in this article by complementing the analysis of common wavelet power (CWP, called WCS in their article) by that of wavelet coherence (called WCO in Maraun and Kuhrts 2004). In the significance analysis for common wavelet power, we use the Monte-Carlo approach of randomizing only one of the two time series, the explanatory one, and not both. This overcomes the problem discussed in the quoted paper that peaks in the common wavelet power caused by one of the two time series only are considered significant.
We will refer to the suggested publication and point this out more clearly.

7. Do the authors give proper credit to related work and clearly indicate their own new/original contribution?
proper credit to related work is only given fairly; in my opinion the overall literature work for the paper could be improved; there is a strong focus on papers that focus mostly on runoff as a driver; however, as the authors claim to explain the investigated interdecadal salinity changes and they also directly investigate on variations in saline inflows/transports and wind-induced mixing, their literature work should be more substantial on what is actually known about drivers behind salinity variations; spontaneously, I can think of works by Schimanke (e.g. 10.1175/JCLI-D-15-0443.1) and e.g. Gustafsson and Andersson (10.1029/2000JC000593); there is also work focusing on improving the conceptual understanding of major Baltic inflows and ultimately Baltic Sea salinity, but unfortunately these are published only as conference talks (e.g. 10.5281/zenodo.3536232 and 10.5281/zenodo.3567086)
Thanks a lot for these suggestions!
We will improve the introduction section and include the suggested references.

8. Does the title clearly reflect the contents of the paper?
not really; the title suggests an analysis of variations in a hindcast simulation only, however, variations in observational records are also studied; furthermore, there are not really many satisfying explanations given, at least not in a conclusive and nicely summarized way; generally I think the manuscript would benefit from focusing on fewer aspects, that should then be tackled more deeply

Even though we do not reach a final explanation yet, we think that the results we have are already worth publishing to support future research on the subject and reach "satisfying explanations". The hindcast simulation with its completeness in time is the major ingredient for the analyses, but it is clear that we also have to take observational data into account.
We change the title to "Investigating drivers of interdecadal salinity changes in the Baltic Sea in a 1850-2008 hindcast simulation" to make clear we do not end up with a final explanation.

10. Is the overall presentation well structured and clear?
mostly; however, in my opinion the authors should better decide on what their actual research questions are; they open many boxes, but do not properly "close" them; the manuscript appears very unfocused to me
The manuscript focuses on two things: (a) using wavelet coherence analysis to show that both runoff and inflows are possible drivers of the 30-year oscillations while AMO and NAO are not and (b) showing that the direct-dilution effect of river runoff is small.
We will add a table summarizing the main findings of the wavelet analysis to better concentrate the results that are scattered across the sub-sections now.

13. Should any parts of the paper (text, formulae, figures, tables) be clarified, reduced,combined, or eliminated?for better focus, e.g. - leave out Figure 3, climate indices analysis, ... - extend "directdilution effect" discussion/analysis, ..
We think the result that wavelet analysis excludes the climate indexes as drivers of the 30-year oscillations is valuable, we want to keep it.
We move Figure 3 to Appendix D and extend the discussion of the direct dilution effect results.

Explaining Investigating interdecadal salinity changes in the Baltic Sea in a 1850-2008 hindcast simulation

Hagen Radtke[1], Sandra-Esther Brunnabend[1], Ulf Gräwe[1], and H. E. Markus Meier[1,2]

[1]Department of Physical Oceanography and Instrumentation, Leibniz Institute for Baltic Sea Research Warnemünde, Rostock, Germany
[2]Department of Research and Development, Swedish Meteorological and Hydrological Institute, Norrköping, Sweden

Correspondence: Hagen Radtke (hagen.radtke@io-warnemuende.de)

Abstract. The detection of historical long-term trends is often complicated by interdecadal Interdecadal variability in the time series of interest. A mechanistic understanding of the causes of this variability allows to separate the signals. Salinity of the Baltic Sea contains a dominant salinity of the Baltic Sea is dominated by a 30-year cycle with a peak-to-peak amplitude of around 0.4 $\mathrm{g\,kg^{-1}}$ at the surface. Such changes may have substantial consequences for the ecosystem, since species are adapted to a suitable salinity range and may experience habitat shifts. It is therefore important to understand the drivers of such changes. We use both analysis of empirical data and a numerical model reconstruction for the period of 1850–2008 to explain these changes. interdecadal changes. The model explains 93% and 52% of the variance in the observed interdecadal salinity changes at the surface and the bottom, respectively, at an oceanographic station at Gotland Deep. It is known that the 30-year periodicity coincides with a variability in river runoff. Periods of enhanced runoff are followed by lower salinities. We demonstrate, however, that the drop in mean salinity cannot be understood as a simple dilution of the Baltic Sea water by freshwater. Rather, the 30-year periodicity in river runoff occurs synchronously with a substantial variation in salt water import across Darss Sill. Fewer strong inflow events occur in periods of enhanced river runoff. This reduction in the import of high-salinity water is the main reason for the freshening of the water below the permanent halocline. In the bottom waters, the variation in salinity is larger than at the surface. As a consequence, the surface layer salinity variation is caused by a combination of both effects, a direct dilution by river water and a reduced upward diffusion of salt as a consequence of reduced inflow activity. Our findings suggest that the direct dilution effect is responsible for 27% of the salinity variations only. It remains unclear whether the covariation in river runoff and inflow activity are only a spurious coincidental correlation during the historical period, or a mechanistic link exists between the two quantities, e.g. both are caused by the same atmospheric patterns.

1 Introduction

The Baltic Sea is a brackish sea with pronounced salinity gradients, both in the horizontal and in the vertical. The narrow and shallow Danish Straits connect this marginal sea via the Kattegat to the adjacent North Sea, which allows a limited exchange of volume and salt. The brackish salinities in the Baltic Sea are the consequence of (i) a positive freshwater balance due to river runoff and net precipitation, (ii) an import of saline water across the shallow Drogden Sill and Darss Sill and (iii) mixing processes inside the Baltic Sea.

Changes in any of these controlling factors may thus affect the Baltic Sea salinity. Major ecological consequences may result from that, since the ecosystem of the Baltic Sea is adapted to the brackish salinities and their horizontal gradient. Species diversity shows a minimum at salinities around 5-8 $\mathrm{g\,kg^{-1}}$ (Khlebovich, 1969), since few marine species, but also few freshwater species can adapt to these salinities. A change in Baltic Sea salinity means a regional shift of this isohaline with corresponding spatial shifts in habitats. Since a freshening of the Baltic Sea is expected in future climate due to enhanced precipitation in the catchment, these regional shifts are expected (MacKenzie et al., 2007; Vuorinen et al., 2015).

The intensity of these future changes will be controlled by the sensitivity of the Baltic Sea salinity to river runoff, i.e. on the vulnerability of the present-day equilibrium salinities towards changes in freshwater supply. Attributing past variations in Baltic Sea salinity is therefore essential to understand the mechanisms behind these and e.g. discriminate between the influences of runoff and wind. If runoff is the main driver of salinity changes, enhanced river runoff will lead to a strong freshening in future climate, whereas if wind patterns and correspondingly the frequency or intensity of salt water inflows are the major cause of salinity fluctuations, future freshening may be weaker.

Separating the influence of runoff and wind on multidecadal salinity fluctuations in the Baltic Sea is the prerequesite for the attribution of these fluctuations to atmospheric driving mechamisms. When these fluctuations can be quantitatively explained, long-term salinity trends caused by different drivers such as sea level rise will be more easily detectable in the historical salinity record.

Both empirical and numerical model studies have assessed the effect of river runoff on Baltic Sea salinity. The studies of Winsor et al. (2001) and of Meier and Kauker (2003a) stressed that the freshwater content of the Baltic Sea showed very similar decadal fluctuations to the accumulated river runoff and net precipitation anomaly, both in phase and magnitude. A Knudsen-like model was employed by Rodhe and Winsor (2002) to explain this strong correlation (corrected in Rodhe and Winsor, 2003). They concluded that enhanced freshwater input would lead to outflow of Baltic Sea water into the Kattegat. This would cause enhanced entrainment of low-saline water into the Kattegat deep water, which enters the Baltic Sea during inflows. A long-term change of 1% in freshwater supply should thus lead to relative changes in salinity of more than 2%. Their model was based on the assumption that relative variations in the barotropic flow through the Danish Straits were much smaller than those in the freshwater input and uncorrelated to them on a 5-years time scale. A steady-state model by Meier and Kauker (2003a) estimated a smaller relative salinity change of 1.6% for a 1% change in runoff. The model was based on the assumption that an increase in runoff leads to a small weakening of the overturning circulation only, and the analytical model results were confirmed by sensitivity experiments of a numerical model.

Another explanation for salinity changes that has been discussed is the intensity variation of westerly winds. On a time scale between 35 and 200 days, Gustafsson and Andersson (2001) found a positive correlation between (a) Kattegat sea level and salinity and (b) the north-south gradient of air pressure across the North Sea, which is directly related to westerly winds. They could show that the salt transports across the sills, derived by a simple conceptual model driven by this pressure gradient, partly explained the observed salinity variations. This explanation was extended by Höflich et al. (2018), who investigated events of large volume transports into the Baltic Sea, which are wind-driven. They demonstrated that the salt import during such events depends on both intensity and rapidness of the volume flow. Stagnation periods with a decade-long drop of salinity were characterized by a lack of volume changes being both large and rapid.

On a multi-year scale, in contrast, stronger westerly winds cause lower salinities (Zorita and Laine, 2000). This effect is partly related to the runoff signal, since stronger westerlies cause higher moisture transport and lead to higher precipitation in the Baltic Sea catchment. Another discussed mechanism is that the resulting barotropic pressure gradient (higher sea level in the Baltic Sea) prevents large barotropic inflows. The study of Schimanke and Meier (2016) discriminated the two effects in a stepwise multilinear regression, using a synthetic 1000-year climate model simulation as input. Here they showed that 44% of the variance in the 10-year lowpass-filtered salinity could be explained by river runoff and precipitation alone, 23% could be explained by zonal wind alone, and 48% could be explained by a combination of all these drivers. This illustrates the strong interdependence between zonal wind and freshwater input.

Past salinity variations in the Baltic Sea show a prominent 30-year cycle, which is known for decades (Malmberg and Svansson, 1982). A similar periodicity exists in river discharge of major Baltic Sea rivers (Meier and Kauker, 2003b; Gailiušis et al., 2011), and a link between both has been discussed (Malmberg and Svansson, 1982). ~~Still it is questionable whether~~ This does, however, not necessarily mean that the salinity variations are caused by a direct dilution effect. Dilution means that an enhanced import of freshwater implies an enhanced export of brackish water, reducing the mass of salt. Another 30-year cycle does, however, show up in the mass of salt imported across Darss Sill during barotropic inflow events (Mohrholz, 2018). These episodically occurring events are responsible for about half of the salt import into the Baltic Sea and are caused by favourable wind conditions ~~(Lass and Matthäus, 1996)~~(Lass and Matthäus, 1996; Höflich et al., 2017). So, it remains unclear which of the variations was the main reason for the observed interdecadal salinity changes. A sensitivity simulation by Meier and Kauker (2003b) showed that decadal variability of Baltic Sea salinity reduced to half when the runoff was replaced by a climatology with no interdecadal variations, suggesting that about 50% of the interdecadal salinity fluctuations were controlled by runoff in their model.

In this article, we explore the past interdecadal salinity variations and the role of the river runoff for these. We demonstrate that the use of (a) wavelet coherence analyses and (b) a new dataset on barotropic inflow variability ~~allows new perspectives on the~~ suggests that the direct influence of runoff on salinity is limited, while barotropic inflow variability contributes to the interdecadal fluctuations. We complement long-term observations by a numerical model hindcast for the period 1850–2008. ~~Wavelet analysis shows that the 30-year period dominates~~ First, we use wavelet analysis to identify the period dominating the interdecadal salinity variations. We then apply wavelet coherence analysis to ~~show that~~ check whether both freshwater and saltwater import vary at the right frequency and phase to potentially explain these salinity oscillations. Finally, we apply a simple two-layer box model to assess the relative importance of the direct dilution effect.

~~Separating the influence of runoff and wind on multidecadal salinity fluctuations in the Baltic Sea is the prerequesite for the attribution of these fluctuations to atmospheric driving mechamisms. When these fluctuations can be quantitatively explained, long-term salinity trends caused by different drivers such as sea level rise should be more easily detectable in the historical salinity record.~~

The paper is organised as follows: In Section 2, we describe the datasets used and the numerical model applied, as well as the mathematical methods (wavelet analyses and a simple two-layer model to quantify the direct dilution effect). Section 3 shows validation results of the numerical model we used. In Section 4, we present the results of the wavelet power and coherency analyses, which we discuss in Section 5. Section 6 discusses the results of the two-layer box model estimation. The paper ends with conclusions and outlook in Section 7.

2 Material and Methods

2.1 Datasets

We use five datasets for this study, namely (1) temperature and salinity observations from the International Council for the Exploration of the Sea (ICES) oceanographic database, (2) the HIRESAFF v2 atmospheric reconstruction, (3) river runoff from Meier et al. (2018a), (4) a reconstruction of Major Baltic Inflows by Mohrholz (2018) and (5) time series of two climate indices, the North Atlantic Oscillation (NAO, Jones et al., 1997) and Atlantic Multidecadal Oscillation (AMO, Oldenborgh et al., 2009).

2.1.1 ICES S and T observations

The first dataset consists of temperature and salinity measurements in the Baltic Sea between 1877 and 2017 from the ICES oceanographic database (ICES, 2019). We extract these data for a set of oceanographic stations which is shown in Fig. 1. Since especially data in the past are scarce, we increase the data coverage by taking data not only from the exact station location but from relatively large latitude-longitude rectangles around the station. These rectangles are also depicted in Fig. 1, the exact coordinates of the stations and the rectangle corners are given in Appendix A.

The data for the individual stations are irregular in depth and time. To obtain time series for surface and bottom salinity, we select all data from the uppermost 20 m and from the depth range between 90% and 100% of the water depth at the station location, respectively. All measurements from the same day are averaged. Calculating annual or longer-term averages from the time series is not straightforward, since a seasonal sampling bias may occur. To correct for this, we fit a Generalised Additive Mixed Model (GAMM) through the data which explains them as a sum of a smooth decadal variation $s_{Longterm}(t_i)$, a smooth seasonal signal $s_{Seasonal}(\tau_i)$, where i denotes the sampling time within a year, ranging between 0 at January 1st and 1 at the end of December 31st, a constant offset S_0 and residuals ϵ_i, whose temporal autocorrelation is assumed to follow a continuous

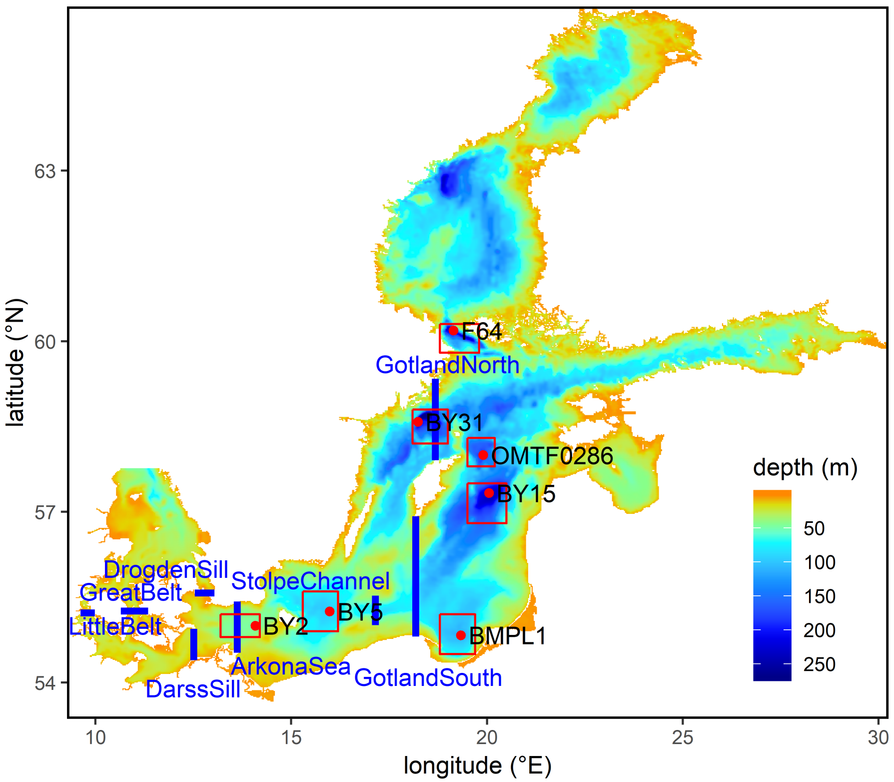

Figure 1. Model topography. Red dots: Oceanographic Stations. Red boxes: Areas around these stations from which ICES observations were selected. Blue lines: Transects across which transports were calculated.

AR(1) model,

$$S_i = s_{Longterm}(t_i) + s_{Seasonal}(\tau_i) + S_0 + \epsilon_i \,. \tag{1}$$

By investigating the autocorrelation of the normalised residuals, we check whether this autocorrelation model is applicable. We use the function gamm from the R package mgcv to fit the model by a restricted maximum likelihood approach. The functions $s_{Longterm}$ and $s_{Seasonal}$ are defined as penalised cubic (and cyclic cubic) regression splines. We allow one degree of freedom per decade for $s_{Longterm}$ and one degree of freedom per month for $s_{Seasonal}$. By subtracting the climatological seasonal salinity signal from the observations, we obtain the deseasonalised salinities as

$$S_i^{corr} = S_i - s_{Seasonal}(\tau_i) \,. \tag{2}$$

These are used to calculate annual and decadal means for surface and bottom salinity at each station.

2.1.2 HIRESAFF v2 atmospheric reconstruction

The second dataset is the HIRESAFF v2 atmospheric reconstruction for the period 1850–2008 (Schenk and Zorita, 2012). This is a reconstruction of past atmospheric states by the analog method (AM). A comparison of the wind speed statistics in the dataset with observed winds at a set of Swedish coastal stations (Höglund et al., 2009) revealed, however, that strong wind speeds were occurring less frequently in the atmospheric reconstruction than in the observations. We therefore corrected the wind speeds by the following piecewise linear formula

$$u_{new} = u_{old} + u_0 \cdot \min\left(u_{old}/u_1, 1\right) \quad (3)$$

where $u_0 = 0.7\,\mathrm{m\,s^{-1}}$ is the correction for strong winds and $u_1 = 4.9\,\mathrm{m\,s^{-1}}$ is the threshold velocity above which this correction is fully applied.

We use the atmospheric data to drive the ocean model, but we also use the third power of the wind speed as a proxy for wind energy input into the ocean, where part of it is transformed into turbulent kinetic energy. From the 10-m wind speeds u_{10} and v_{10} given in the atmospheric forcing dataset, we calculate the third power of the wind speed as $u^3 = \sqrt{u_{10}^2 + v_{10}^2}^3$. We obtain a time series for each oceanographic station listed in Section 2.2 by averaging this value over the corresponding rectangle shown in Fig. 1 and whose coordinates are given in Appendix A. The motivation to use the third power of the wind speed is that the wind work, i.e. the kinetic energy input by wind, scales with the third power of the wind.

This HIRESAFF atmospheric dataset has been successfully applied for model-based Baltic Sea reconstructions in the past. The basin-integrated BALTSEM model was applied by Gustafsson et al. (2012) and a 2 n.m. RCO model was used by ~~Meier et al. (2012, 2018a)~~Meier et al. (2012, 2018b). These studies, however, had their focus on the reconstruction of marine biogeochemistry. Two different ocean models (MOM and RCO, 3 and 2 n.m. resolution, respectively) were used by Kniebusch et al. (2019) to investigate Baltic Sea temperature variability over the 1850–2008 period.

2.1.3 River runoff

The third dataset describes monthly river runoff which we adopt from a previous model study (Meier et al., 2018a). Monthly river discharges were merged in time from different sources, i.e. reconstructions by Hansson et al. (2011) for 1850–1900, Cyberski et al. (2000) for 1901–1920 and Mikulski (1986) for 1921–1949, observations from the BALTEX Hydrological Data Center (BHDC) (Bergström and Carlsson, 1994) for 1950–2004, and hydrological model results Graham (1999) for 2005–2008. We choose the ArkonaSea transect (see Fig. 1) and aggregate the runoff of the Baltic Sea rivers eastward of the transect to obtain a cumulated runoff time series.

2.1.4 Baltic Inflow reconstruction

The fourth dataset is a reconstruction of Baltic Inflows by Mohrholz (2018). For 1426 barotropic inflow events of different strength between 1887 and 2018, the inflowing mass of salt (in Gt) across Darss and Drogden Sill was reconstructed based on sea level and salinity from the Belt Sea and the Sound and river discharge. These events are differentiated into large inflows (category DS5, indicating that a threshold salinity was exceeded for at least five consecutive days at Darss Sill) and smaller ones. For each of these categories, we obtain three annual time series: (a) total mass of imported salt, (b) number of events during the year, (c) average strength of the events during the year. For those years where no events occurred, we use linear interpolation in time series (c) to fill the gaps. This may lead to an overestimation of inflow strength when years with strong inflows are followed by years without inflow activity, but we need to generate a complete time series to apply the wavelet analysis method.

2.1.5 Climate indices

Finally, the fifth dataset consists of the climate indices AMO and NAO. The NAO is a dimensionless index traditionally describing the anomaly of the surface pressure difference between the Azores and Iceland. We use a dataset based on the pressure difference between Gibraltar and Iceland (Jones et al., 1997) extending backwards until 1821. The AMO index describes a sea surface temperature (SST) anomaly of the Northern Atlantic. We use an AMO index calculated from the SST in the latitude-longitude range of 25–60°N and 7–75°W minus a regression on the global mean temperature as described by Oldenborgh et al. (2009), based on the Hadley Center SST dataset HadSST 3.1.1.0 (Kennedy et al., 2011a, b). Both datasets were downloaded from the Royal Netherlands Meteorological Institute (KNMI) climate explorer dataset collection (KNMI, 2019).

2.2 Model simulation

We use two models in the study, a 3-d hydrodynamic model and a box model. This section is about the 3-d model, the box model is described in Section 2.5.

Salinities and salt transports for the period 1850–2008 are obtained from a hindcast simulation with the General Estuarine Transport Model (GETM, www.getm.eu). This hydrodynamic model solves the hydrostatic Boussinesq equations on a regular latitude-longitude grid with approximately 1 $\mathrm{n.m.}$ horizontal resolution. The model topography (see Fig. 1) is based on the iowtopo bathymetry (Seifert et al., 2001) but has been smoothed to reduce numerical mixing. Manual corrections were applied in the Danish Straits where the grid resolution only allows a rough representation of the topographic features. In the vertical, the model has 50 layers with vertically adaptive coordinates (Gräwe et al., 2019). Compared to traditional z- or σ-coordinates, these allow a higher resolution in the proximity of pronounced density gradients, which reduces numerical mixing. More details on the model setup can be found in Appendix C.

Our model was integrated for 159 years, from 1850 to 2008. Atmospheric forcing conditions are prescribed from the HIRESAFF v2 dataset (Schenk and Zorita, 2012) which spans this period. Reconstructed river runoff and open boundary conditions for the simulation period were adopted from a previous model study (Meier et al., 2018a).

For the comparison of time series between model and observations, we use the classical measure of explained variance, defined as (e.g., Good and Fletcher, 1981)

$$\rho^2 = \frac{\sigma_{obs}^2 - \sigma_{res}^2}{\sigma_{obs}^2}. \quad (4)$$

Here, σ^2_{obs} is the variance in the observations and σ^2_{res} is the variance in the residuals, i.e. the difference between observations and model. The explained variance is one if and only if the residuals vanish. It is typically between zero and one but can also become negative if there is an anticorrelation between model and observations.

2.3 Salinity-discriminated transports

Salt and volume transports as well as mean salinities were stored in daily resolution at selected transects for each grid point and vertical layer. From these data, transports per salinity interval were calculated, following the Total Exchange Framework (TEF) analysis framework (Walin, 1977, 1982; MacCready, 2011; Burchard et al., 2018). The procedure is as follows: In a first step, we define salinity limits every 0.025 $\mathrm{g\,kg^{-1}}$ between 0 and 36 $\mathrm{g\,kg^{-1}}$. For each of these salinity limits, we calculate the sum of transports over all grid cells and vertical layers with a mean salinity above this limit,

$$T_{S^*,t} = \sum_i \sum_k T_{i,k,t} \cdot \theta\left(S_{i,k,t} - S^*\right), \quad (5)$$

where $T_{i,k,t}$ denotes the salt transport across the transect in grid cell i and layer k during time step t, $S_{i,k,t}$ denotes the average salinity in this grid cell, layer and time step, S^* is the salinity limit above which the transport is measured, and θ denotes the Heaviside step function, $\theta(x) = 1$ for $x > 0$ and $\theta(x) = 0$ otherwise. It should be noted that while the total transports across the transect are exactly conserved, their attribution to the salinity bins contains some uncertainty depending on the model output frequency. The transports are counted positive if they are directed into the Baltic Sea.

Let us consider the time-averaged salinity-discriminated transports T_{S^*} as a function of S^*. These have a typical shape as shown in Fig. 2: They are zero at high salinities, show a maximum at a value $\hat{S}$ which depends on the cross section, and then decrease again as salinity approaches zero. This reflects the fact that net inflow occurs on average for salinities above $\hat{S}$ (near the bottom), while net outflow occurs at lower salinities (near the surface). The value $\hat{S}$ denotes the salinity class where inflow and outflow compensate for each other. We can then derive salinity quantiles of the net import and net export as shown in Fig. 2. The value $S_{in}^{p\%}$ shall define the salinity above which $p\%$ of the net inflow occurs, it can be determined from the salt transports by

$$T_{S_{in}^{p\%}} = \frac{p}{100} \cdot \hat{T} \text{ and } S_{in}^{p\%} \geq \hat{S}. \quad (6)$$

We determine two time series for net imports across each transect,

$$T_{highsal,t} = T_{S_{in}^{50\%},t} \quad (7)$$

denotes the net import in the high-salinity range, while

$$T_{\hat{S},t} = T_{S_{in}^{100\%},t} \quad (8)$$

denotes the net import at all salinities above $\hat{S}$. The import at low salinities, $T_{lowsal,t}$, is the difference between the two.

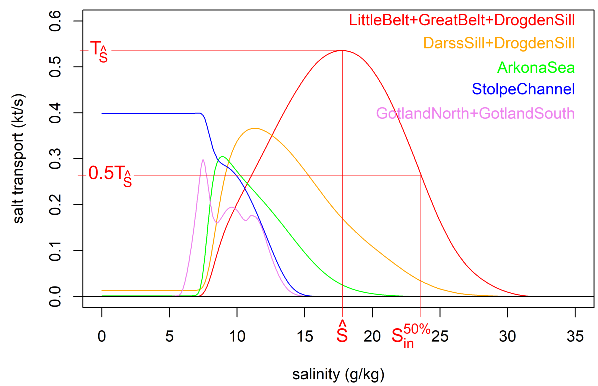

Figure 2. Net salt transports into the Baltic Sea above a specific salinity level, temporal average across the simulation period 1850–2008. Most curves tend to values close to zero at low salinities, indicating that no systematic salt gain or loss occurs inside closed transects. Stolpe Channel and DarssSill+DrogdenSill transects are not closed, the latter due to the existence of the Storstrømmen channel in the model.

2.4 Wavelet analysis

Summarising the above sections, we obtained the following collection of time series which start in the 19th century with at least annual resolution:

- Modelled surface/bottom salinity, for each oceanographic station (from 3-d model)
- Third power of the wind speed as a proxy for wind work, for each oceanographic station (Schenk and Zorita, 2012)
- Three time series for net salt transports into the Baltic Sea ($T_{highsal,t}$, $T_{lowsal,t}$, $T_{\hat{S},t}$), for each transect (from 3-d model)
- Salt import, inflow frequency and strength reconstructed by Mohrholz (2018) for Darss Sill
- River runoff into the Baltic Sea, inside the ArkonaSea transect (Meier et al., 2018a)
- The two most prominent climate indices for Europe, NAO and AMO (KNMI, 2019).

To find out at which time scales the variations in the time series occur, we investigate them with the wavelet analysis method. To explore the correlations between different time series in specific frequency bands, we apply wavelet coherence analysis.

Wavelet analysis is a generalisation of Fourier analysis and also aims at separating signals in different frequency ranges. In Fourier transform, we use the highest possible frequency resolution, which is determined by the step width of the time series under investigation. The amplitude for each frequency range is then calculated by a convolution of the time series with an infinite harmonic function. The price for the high frequency resolution is the loss of all temporal information, which is then only stored in the Fourier phases. In a wavelet transform, we calculate the convolution with time-limited functions. The Morlet wavelet we use ~~(Fig. D1)~~ has the shape

$$\phi(a,t) \quad = \quad \frac{\sqrt{2}}{\sqrt{\pi}a} \exp\left(-i\omega_0 \frac{t}{a}\right) \exp\left(-\frac{t^2}{2a^2}\right), \tag{9}$$

where a is the wavelet width (in time units) and ω_0 is a dimensionless shape parameter which controls whether the resolution of the wavelet analysis is higher in the frequency range or the temporal range. The wavelet transform is calculated as

$$W(a,t) \quad = \quad \int_{\tau=-\infty}^{\infty} d\tau x(\tau)\phi(a,t-\tau). \tag{10}$$

~~The Morlet wavelet for the temporal scale $a = 1$ and $\omega_0 = 6$. Solid line: real part. Dashed line: imaginary part. Please note that the periodicity almost matches the temporal scale.~~

For analysing whether two time series $x(t)$ and $y(t)$ share energy in a specific frequency band at the same time, we calculate common wavelet power (CWP) and wavelet coherence. Common wavelet power is just the product of the wavelet amplitudes,

$$\mathrm{CWP}(a,t) \quad = \quad |W_x(a,t)W_y(a,t)|. \tag{11}$$

If we consider $x(t)$ as the time series to be explained and $y(t)$ as a possible driver of it, we normalise the latter time series by dividing through its standard deviation such that the common wavelet power has the same unit as the original time series $x(t)$. Wavelet coherence is a measure which determines how stable the relative phase between two time series around a specific point in the time-frequency plane is. As pointed out by Maraun and Kurths (2004), an interrelation between two time series should not only be identified by strong CWP but also by a stability in the phase difference. Details on the wavelet calculations can be found in Appendix D. To assess whether the correlations identified with the wavelet methods are significant, we compare the magnitudes of $W(a,t)$ and $\mathrm{CWP}(a,t)$ against those of surrogate time series which were created by block-shuffling complete years in the individual time series. Where the magnitudes exceed those of 95% of the surrogate time series, we consider them as significant.

2.5 Salt budget calculations to estimate the direct dilution effect

A budget method is used with the aim to discriminate between salinity changes due to direct dilution by river water and reduced salt import into the Baltic Sea. We separate the water volume of the Baltic Sea inside the ArkonaSea transect by an isohaline at a constant salinity $S_{isohaline}$. We then calculate time series for the volume V and salt mass s both above and below the isohaline. The volume and salt fluxes into and out of the compartments are denoted in Fig. 3.

From the volume and salt budget of the water body below the isohaline, we can calculate the upward transport of volume and salt into the overlying water:

$$Q^s_{up} \quad = \quad Q^s_{bottom} - \frac{d}{dt} s_{bottom}, \tag{12}$$

$$Q^V_{up} \quad = \quad Q^V_{bottom} - \frac{d}{dt} V_{bottom}. \tag{13}$$

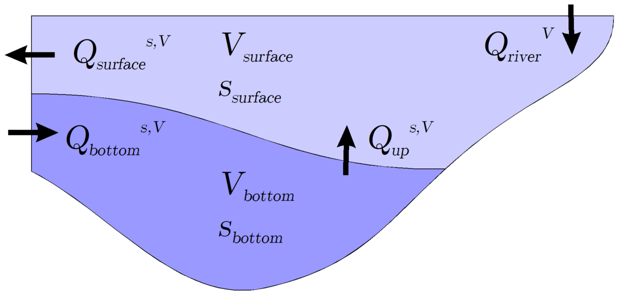

Figure 3. Schematic view of salt and volume fluxes in and out of two compartments, separated by an isohaline. The volumes V and salt masses s inside these compartments change over time.

In a similar way, we can calculate the export across the transect in the overlying water:

$$Q^s_{surface} = Q^s_{up} - \frac{d}{dt} s_{surface}\,, \tag{14}$$

$$Q^V_{surface} = Q^V_{up} + Q^V_{river} - \frac{d}{dt} V_{surface}\,. \tag{15}$$

We assume that the surface salt export is approximately determined from volume export and the surface salinity, we derive an approximation by

$$\tilde{Q}^s_{surface} = \alpha \frac{Q^V_{surface} s_{surface}}{V_{surface}}\,, \tag{16}$$

where the parameter α accounts for horizontal inhomogeneity in the salinity, it is determined by a least-squares fit of $\tilde{Q}^s_{surface}$ to $Q^s_{surface}$. (The error by the simplification of choosing a constant α will be discussed *a posteriori*.) If we insert the approximation (16) into (14), we obtain a differential equation for $s_{surface}$ as follows:

$$\frac{d}{dt} s_{surface} = Q^s_{up} - \alpha \frac{Q^V_{surface} s_{surface}}{V_{surface}} \tag{17}$$

Here we can see how a direct dilution effect may affect the salinity: A higher river runoff enhances the outflow volume $Q_{surface}$ and leads to a sinking salinity. The solution of the differential equation reads

$$s_{surface} = A(t) \left(\int_{t_0}^{t} \frac{Q^s_{up}}{A(t')}\, dt' + C_1 \right) \tag{18}$$

with

$$A(t) = \exp\left(- \int_{t_0}^{t} \frac{Q^V_{surface}}{V_{surface}}\, dt' \right)\,. \tag{19}$$

We prescribe the initial salt content, which fixes the integration constant C_1 at

$$C_1 = s_{surface}(t_0)\,. \tag{20}$$

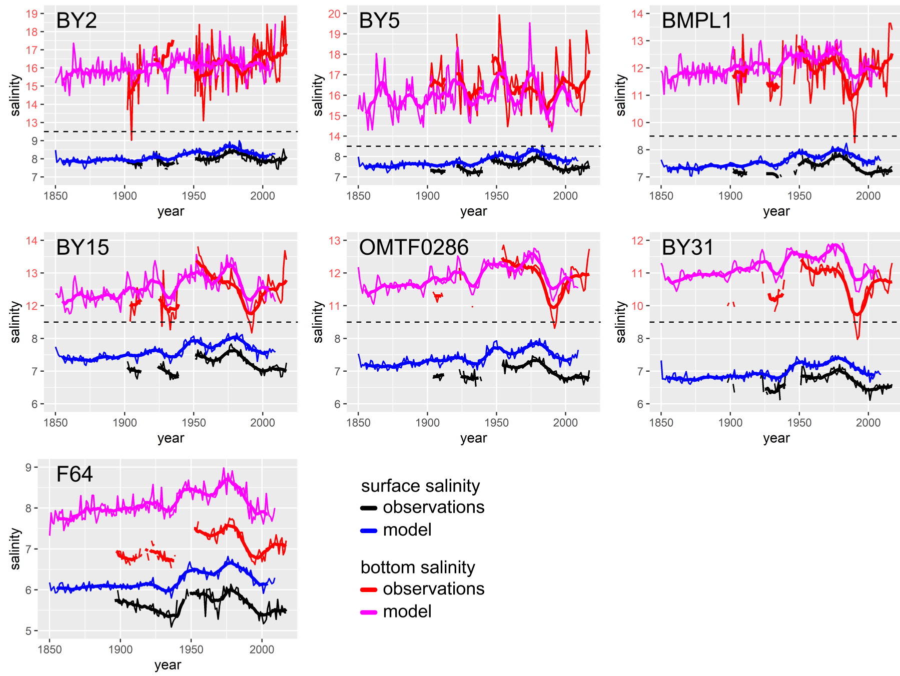

Figure 4. Surface and bottom salinity at selected oceanographic stations from observations and model. Thin lines: annual averages. Thick lines: 11-year running mean. Data are corrected for seasonal observation bias. Running mean is shown where at least 6 years of data were available. Dashed lines and red axis annotations indicate a broken salinity axis for better visibility.

To calculate the solution of the differential equation, we use annual means of the fluxes across the ArkonaSea transect and of the volumes and salt contents above and below the halocline. The solution of this simplified salinity estimator is compared to the results of the full model to prove the applicability of the method. After this has been shown, we solve the equation again for a temporally constant river runoff, but keeping the salt and volume fluxes through the halocline constant. The difference between the two salinity time series then measures the direct dilution effect.

3 ~~Model~~ Numerical model validation

3.1 Surface and bottom salinity at selected stations

The surface and bottom salinities at the selected stations shown in Fig. 1 are compared to ICES observations from rectangles around the station location. Fig. 4 shows this comparison for annual and 11-year running means of surface and bottom salinity. The comparison shows that a substantial part of the interdecadal variability at most stations is reproduced by the model. Modelled salinities, however, show a positive bias which increases with latitude.

Table 1. Basic statistics for fit between model and observations with respect to surface and bottom salinities

station	decadal mean salinity				annual mean salinity			
	surface		bottom		surface		bottom	
	expl. var. (%)	RMSE ($g\,kg^{-1}$)	expl. var. (%)	RMSE ($g\,kg^{-1}$)	expl. var. (%)	RMSE ($g\,kg^{-1}$)	expl. var. (%)	RMSE ($g\,kg^{-1}$)
BY2	72.4	0.26	12.8	0.71	58.0	0.32	23.6	1.27
BY5	81.0	0.35	-56.4	0.69	68.5	0.39	17.4	1.02
BMPL1	81.3	0.35	52.6	0.42	69.9	0.35	43.7	0.69
BY15	93.0	0.48	51.8	0.39	74.2	0.48	42.1	0.47
OMTF0286	89.5	0.51	55.9	0.38	50.8	0.53	56.9	0.41
BY31	64.2	0.35	57.0	0.70	54.9	0.42	59.0	0.73
F64	38.2	0.59	59.5	1.03	40.7	0.64	54.5	1.12

Table 1 shows the explained variance and the root-mean squared error between model and observations. The model captures the variability in surface salinities better than that of bottom salinities. Especially the decadal variations in surface salinity are well captured by the model, more than 80% of the variance can be explained by the model in the Eastern Gotland Basin and in the Bornholm Basin. For the bottom salinities, the model can explain about half of the variability in the Central Baltic, both in the annual and the decadal means. In the Western Baltic, however, a smaller fraction of the variance is explained, and for the decadal mean at Bornholm Deep (BY5) we even find an anticorrelation between model and observations. We therefore focus on station BY15 when we consider modelled bottom salinities.

The question why the bottom salinities can match better in the Central Baltic compared to the entrance area is discussed in Appendix E.

3.2 Transports across the sills

Volume transport across the DrogdenSill transect was compared to a simple linear model which is based on the sea levels in Klagshamn and Viken, z_K and z_V. From these, the transport can be approximated by

$$T_{Vol} \quad = \quad Q\sqrt{\Delta z'}\frac{\Delta z'}{|\Delta z'|}\,, \tag{21}$$

where

$$\Delta z' = z_K - z_V\,(1 + 0.16\theta\,(z_K - z_V)) \tag{22}$$

is the corrected sea level difference between the two stations, θ denotes the Heaviside step function, and $Q = 74770\,\mathrm{m}^{5/2}\,\mathrm{s}^{-1}$ is an empirical constant (Häkansson et al., 1993). Hourly tide gauge data were downloaded from the GESLA (Global Extreme Sea Level Analysis) portal (https://gesla.org/), and daily volume transports were calculated from them. A comparison to the results

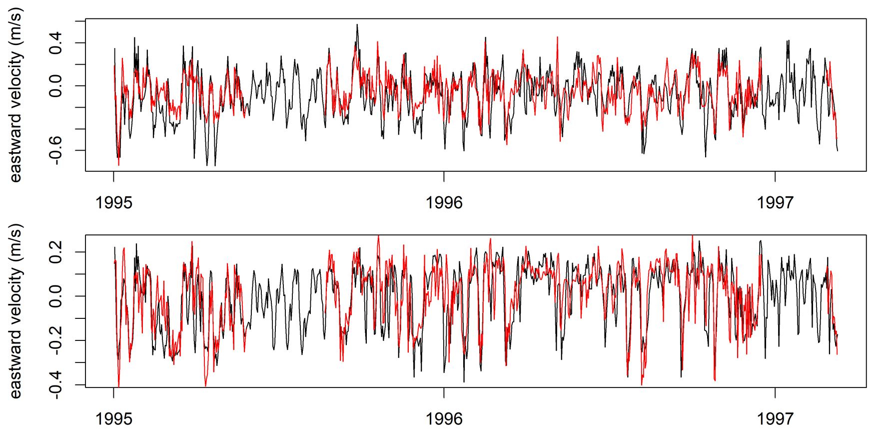

Figure 5. Eastward velocity at Station Darss Sill (54.7°N, 12.7°E), top row: in 3 m depth, bottom row: in 17 m depth. Black line: model results. Red line: ADCP observations.

of the numerical model showed that the model transports had a 24% higher standard deviation, but the correlation coefficient between both time series is $R = 0.766$, which means that $R^2 = 58.6\%$ of the variability was explained by the correlation between them. For the DarssSill transect, we used observations from an acoustic doppler current profiler (ADCP) at a permanent observation station (54.7°N, 12.7°E) and directly compared them to our model velocities at the nearest grid point. Observations were taken from the database of the Leibniz Institute for Baltic Sea Research Warnemünde (https://odin2.io-warnemuende.de), and daily-mean eastward velocities in 3 m and 17 m depth were compared between model and measurements for the period 1995–2008. Figure 5 shows a visual comparison for the first few years. It can be seen that the time series compare reasonably well in most situations, while the model overestimates near-surface peak velocities during outflow situations. The correlation between observed and modelled velocities explains $R^2 = 43.5\%$ and 40.5% of the variance in 3 m and 17 m depth, respectively.

4 Results of wavelet analysis

4.1 Interdecadal changes in salinity

Wavelet analysis of both surface and bottom salinities highlighted a signal with a 30-year periodicity, see Fig. 6 and 7. It becomes prominent in the first half of the 20th century in the model. Since the observations only start in the end of the 19th century, it is impossible to decide whether the signal starts earlier in the observations. For the surface salinities, the signal is significant for all of the considered stations both in the model and the observations. For the bottom salinities, the 30-year signal is present for the stations in the Central Baltic Sea only, it is missing or shifted in frequency in Arkona and Bornholm Sea (stations BY2 and BY5). The signal indicates a fluctuation with an amplitude of 0.2 $\mathrm{g\,kg^{-1}}$ (or 0.4 $\mathrm{g\,kg^{-1}}$ peak-to-peak) in the surface salinity. For the bottom salinities, the strength of the signal varies between 0.5 $\mathrm{g\,kg^{-1}}$ in the Gdansk Deep (Station

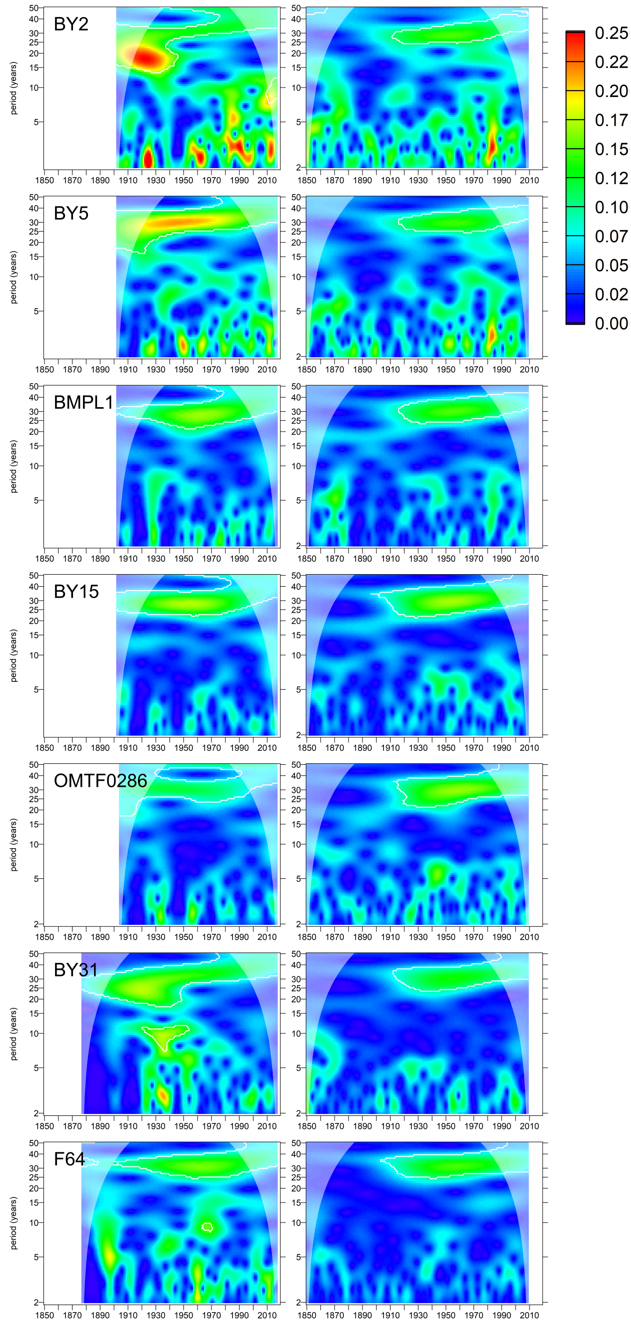

Figure 6. Wavelet amplitudes of surface salinities at selected oceanographic stations (g kg^{-1}). Left column: Observations, right column: Model results. White contours denote significant amplitudes at the 95% confidence level compared to surrogate data randomised by shuffling the years.

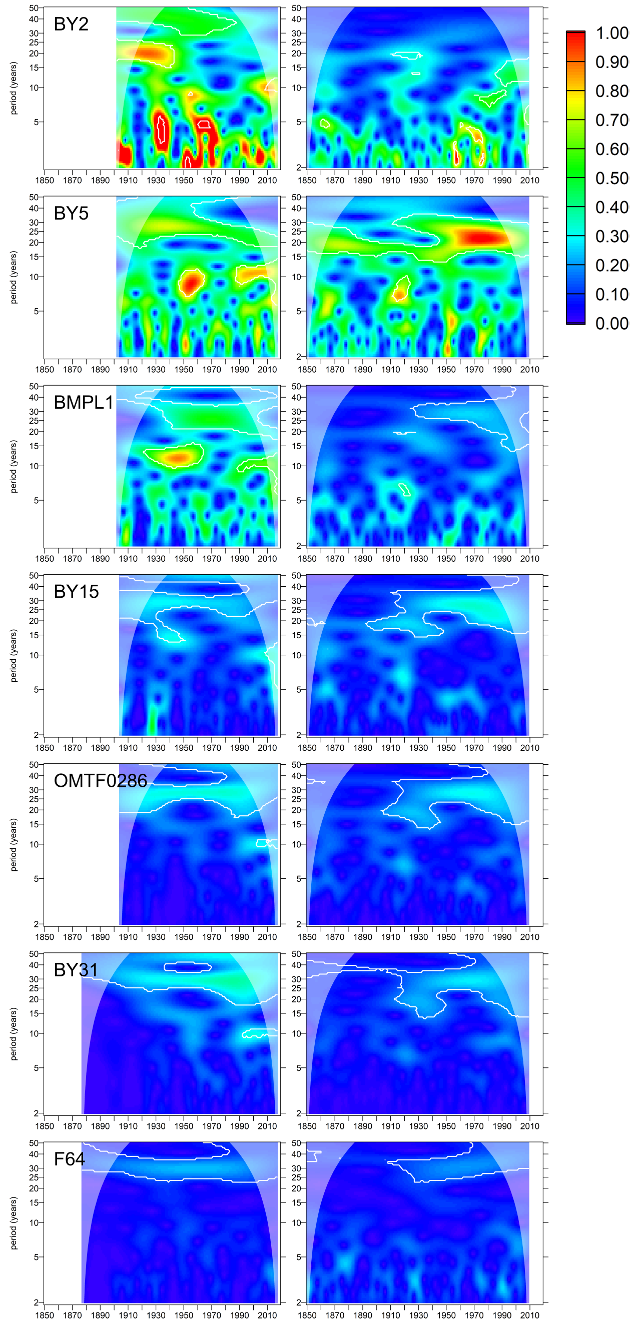

Figure 7. Wavelet amplitudes of bottom salinities at selected oceanographic stations ($\mathrm{g\,kg^{-1}}$). Left column: Observations, right column: Model results. White contours denote significant amplitudes at the 95% confidence level compared to surrogate data randomised by shuffling the years.

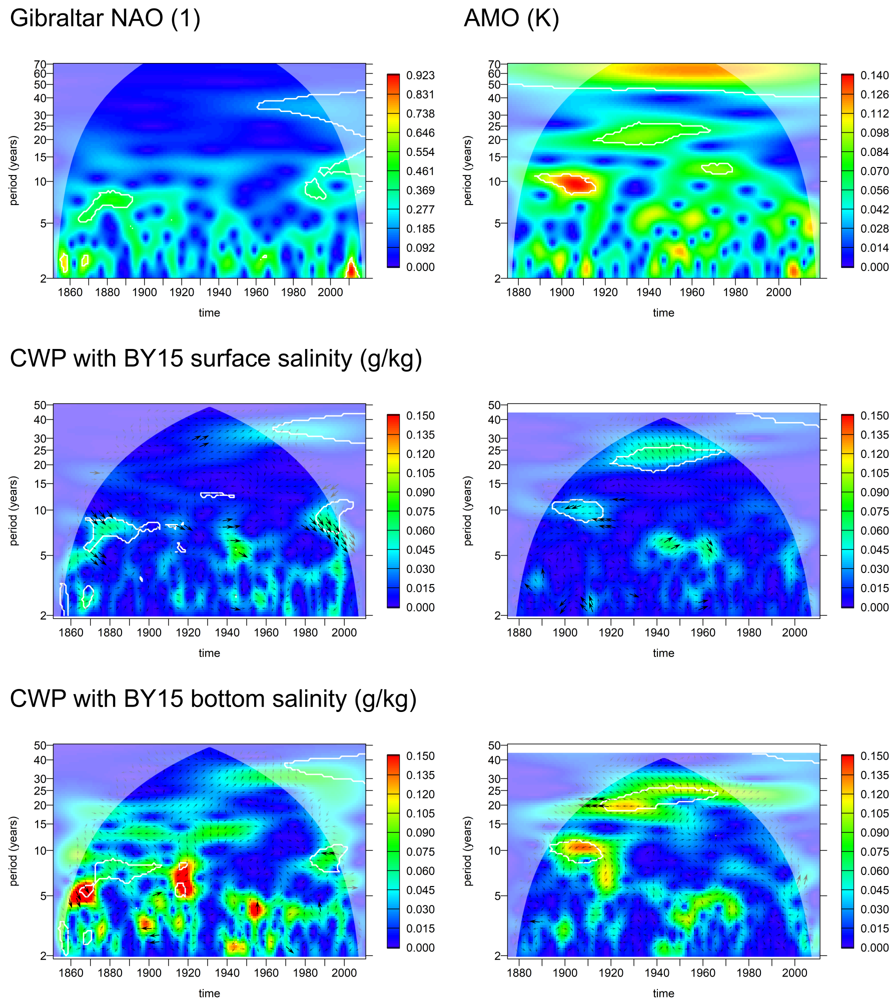

Figure 8. Top row: Wavelet amplitudes (WA) of NAO (Gibraltar-Iceland) and AMO index. Bottom rows: Common wavelet power (CWP) between modelled surface and bottom salinities at station BY15 and the normalised climate indices. White contours indicate that the WA/CWP is significant at the 95% confidence level with respect to a random shuffling of the annual values of the climate index. Arrows indicate relative phase: $\rightarrow$= in phase, $\downarrow$=climate index leading salinity by 90°. Thick arrows indicate phase stability (wavelet coherence > 0.95).

BMPL1) and 0.2 $\mathrm{g\,kg^{-1}}$ at the northernmost station F64. The model slightly underestimates this long-term signal. At some stations, additional significant variability exists at a periodicity of 10 years, however, this signal is episodic.

4.2 Relation to global climate indices

The wavelet decomposition of the NAO and AMO signal (Fig. 8, top row) shows that none of these indices shows the same pattern in the 30-year frequency band as the salinities. In the NAO signal, we find significant energy in this frequency band, but only since the 1960s. In the AMO signal, a 60-year period is pronounced. We also find significant energy (with respect to white noise) in the band around 20–25 years, that is, at the higher range of the frequencies we observe in the salinity time series. This signal is, however, limited in time and no longer significant after the 1970s. To see whether the global climate indices may explain the decadal variability in the salinity signal, we calculate common wavelet power between the modelled salinities at station BY15 and the normalised climate indices (Fig. 8, bottom rows). We find common wavelet power between NAO and the surface/bottom salinity in the range of 0.05 to 0.1 $\mathrm{g\,kg^{-1}}$ around the 30-year frequency band, however, only from 1940 on and not statistically significant. Here, the NAO is slightly lagging the salinity signal with a wavelet coherence below 0.95. Stronger wavelet coherence is found in the frequency band between 5 and 10 years for the periods 1860–1880 and 1980–2000, where the NAO is slightly leading surface salinity at station BY15. Alternative NAO indices were also investigated (Azores-Iceland annual and winter NAO), and no clear correspondence to the 30-years salinity signal was found either (not shown).

For the AMO, we find significant common wavelet power in the 20–25 year band. The phase relation between the signals is, however, changing. For the decade 1910–1920, we find wavelet coherence above 0.95 when AMO and bottom salinity are in anti-phase, however, at a period around 20 years. Later in the 20th century, the relative phase changes in the frequency band between 25 and 30 years, with the negative AMO then slightly leading the salinities in the 1920s to 1940s and later strongly leading it in the 1980s. This holds true for both surface and bottom salinities.

4.3 Processes related to interdecadal salinity changes

4.3.1 River runoff

The total river runoff eastward of the ArkonaSea transect (Fig. 1) has been calculated from the model forcing. Its wavelet decomposition is shown in Fig. 9. We find significant wavelet power from 1910 on in the 30-year frequency band, the oscillations inside a 30-year cycle amount to +/- 6% of the mean runoff for the considered period. There is also significant common wavelet power in this frequency range, the CWP with bottom salinity being larger than that with surface salinity. The relative phase is stable (wavelet coherence mostly above 0.95) wherever common energy exists. In the 30-year frequency band, we find a 90° phase shift (7.5 years lag, slightly less for bottom salinity) between the time series, with negative runoff anomalies leading high salinities. For surface salinities, this relation is stable over the entire 20th century, in the bottom salinity the lag reduces towards the end of the century. For the bottom salinities, we find similar phase relations also in the frequency bands between 3 and 15 years, with always low runoff occurring before high salinities, however, with differing lag time. Using observed instead of modelled salinities gives the same results (not shown).

4.3.2 Frequency versus strength of inflow events

Fig. 10 shows the wavelet decomposition of the salt import across Darss Sill which was caused by the barotropic inflow events found in Mohrholz (2018). Looking at the total import (top left figure), we find strong relative deviations of more than 30% on periods lower than 5 years and smaller deviations on longer time scales, the longest time scale around 30 years on which a relative change of $\pm15\%$ shows up between 1900 and 1990. The relative changes in the salt import by large (DS5 class) inflow

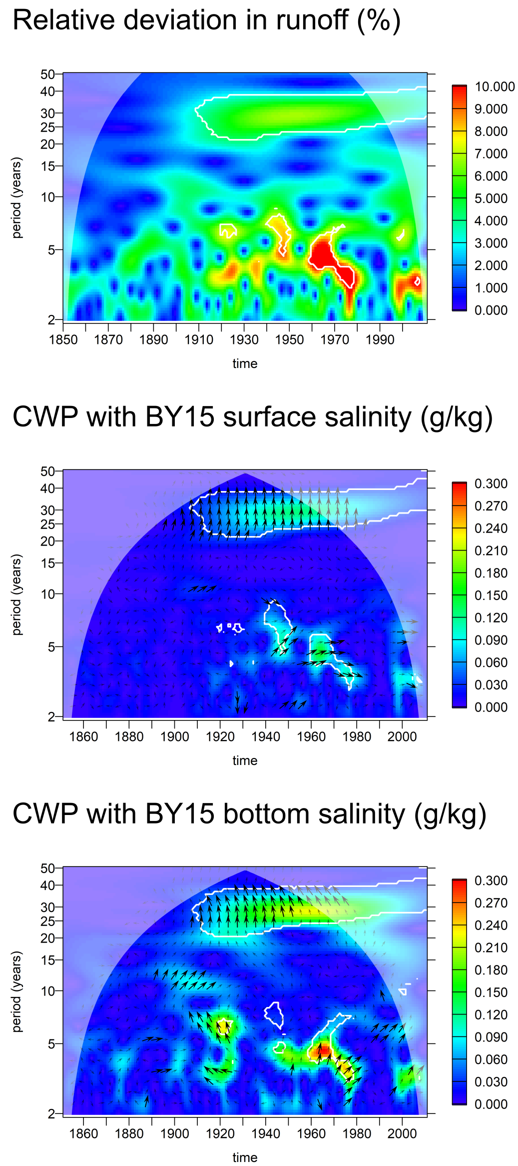

Figure 9. Top row: Wavelet amplitude of the relative deviation in runoff of all model rivers inside the ArkonaSea transect, see Fig. 1. Middle row: Common wavelet power between modelled surface salinity at station BY15 (Eastern Gotland Basin, $\mathrm{g\,kg^{-1}}$) and normalised runoff, note that the scale is doubled from Fig. 8. Bottom row: The same for bottom salinity. White contours indicate that the WA/CWP is significant at the 95% confidence level with respect to a random shuffling of the annual means of the runoff. Arrows indicate relative phase: $\rightarrow$=high runoff and salinity in phase, $\uparrow$=low runoff leading salinity by 90°. Thick arrows indicate phase stability (wavelet coherence > 0.95).

events are stronger and intermittently statistically significant for different periods between 3 and 30 years. The 30-year period shows statistically significant energy between 1940 and 1980.

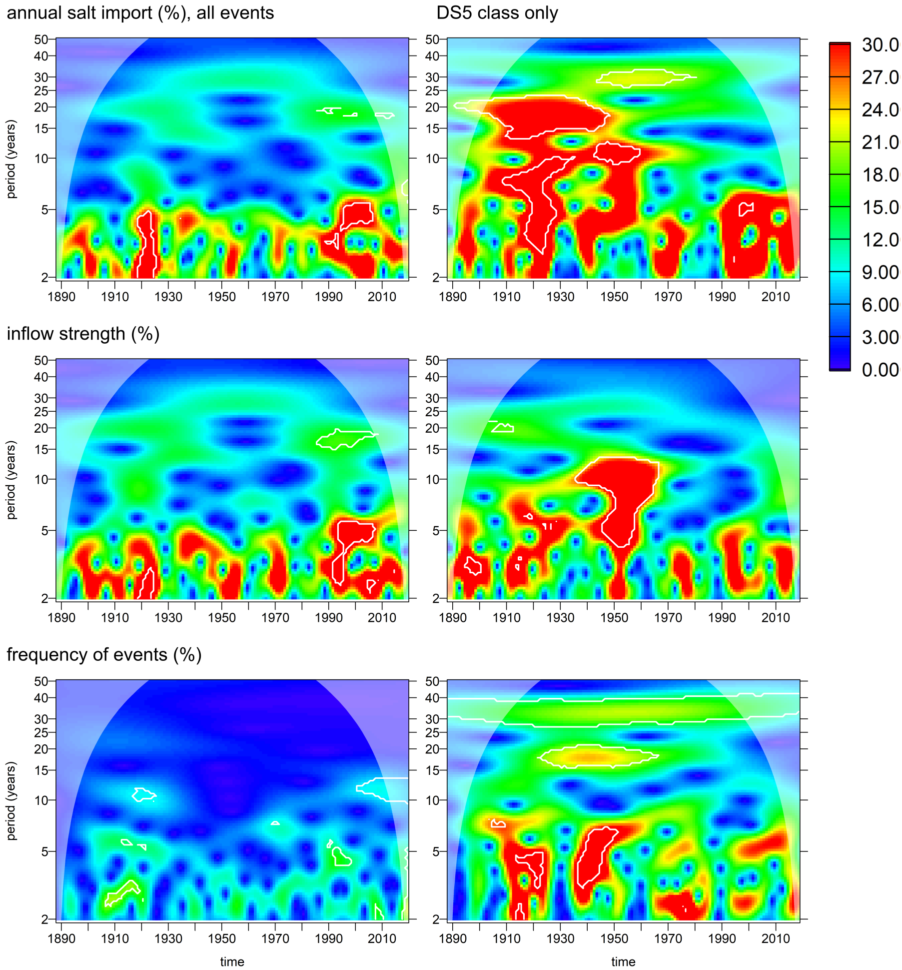

Figure 10. Wavelet analysis of the relative change in inflow activity (%). Top row: total salt import. Middle row: Inflow strength as mean salt import during a single inflow event. Bottom row: Inflow frequency as number of inflows per year.

The salt import is determined both by the frequency of the inflow events and their individual strength in terms of the salt import during a single inflow event. Focussing on the 30-year time scale, we find that a change in inflow strength occurs which is strongest between 1940 and 1980. The total frequency of all inflow events does, however, not change substantially at multidecadal time scales. In contrast, the frequency of strong (DS5 class) inflow events shows a significant variation in the 30-40 year range for the entire period of the analysis.

Fig. 11 shows the common wavelet power which exists between the observed time series of surface and bottom salinity at Gotland Deep and the salt import during the barotropic events identified by Mohrholz (2018). The salt import time series have been normalised (divided by their standard deviation) such that the common wavelet power directly measures the salinity

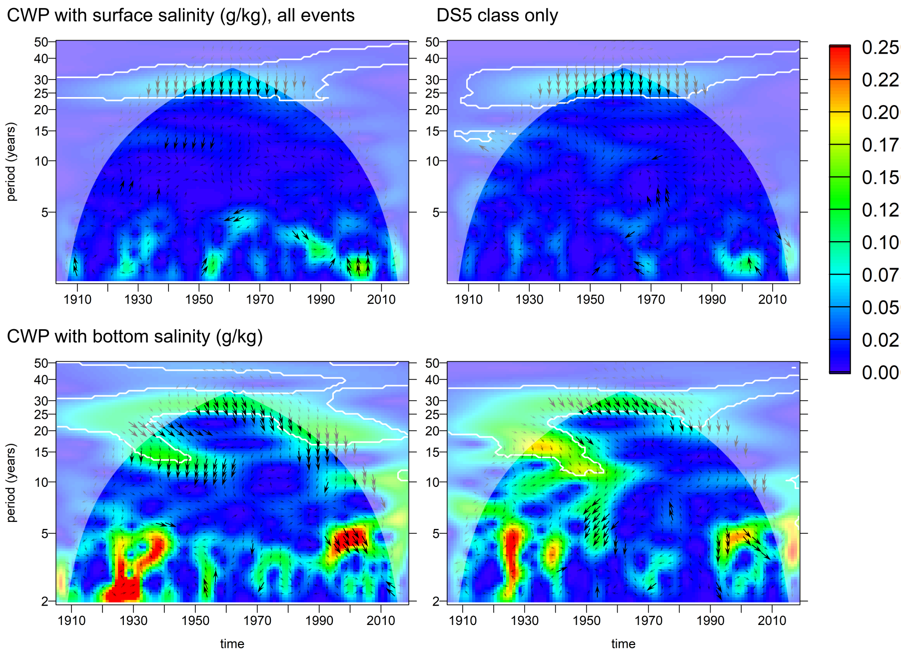

Figure 11. Common wavelet power between observed surface and bottom salinity at station BY15 (Eastern Gotland Basin) and normalised annual import of salt by inflow events. Left column: All inflow events identified in Mohrholz (2018). Right column: Only DS5 class events. White contours indicate that the WA/CWP is significant at the 95% confidence level with respect to a random shuffling of the annual means of the salt import. Arrows indicate relative phase: →= in phase, ↓=salt import leading salinity by 990°. Thick arrows indicate phase stability (wavelet coherence > 0.95). The region where arrows are not drawn indicates the cone of influence for the common wavelet power, the white shading indicates the cone of influence for the wavelet coherence.

deviations related to the fluctuations in salt import. CWP between salt import and bottom salinity (bottom row in Fig. 11) exists intermittently for different periodicities above 10 years. For the 30-year period, the common wavelet power is significant for the entire period in which our analysis is outside the cone of influence. Wavelet coherence above 0.95 is frequently observed, especially at the 30-year period, always indicating that the salt import leads the bottom salinity, but with different lag. For the 30-year period, the lag is around 60° which means approximately 5 years. For the surface salinity, common wavelet power on time scales longer than 5 ears shows up around the 30-year period only. Here, the lag between salt import and salinity maxima is around 7.5 years.

4.3.3 Salt import at high and low salinities

In the following, model results are discussed instead of observations. Fig. 12 shows a wavelet decomposition of the modelled salt imports in different salinity ranges across different transects in the model. We consider the import in the full salinity range

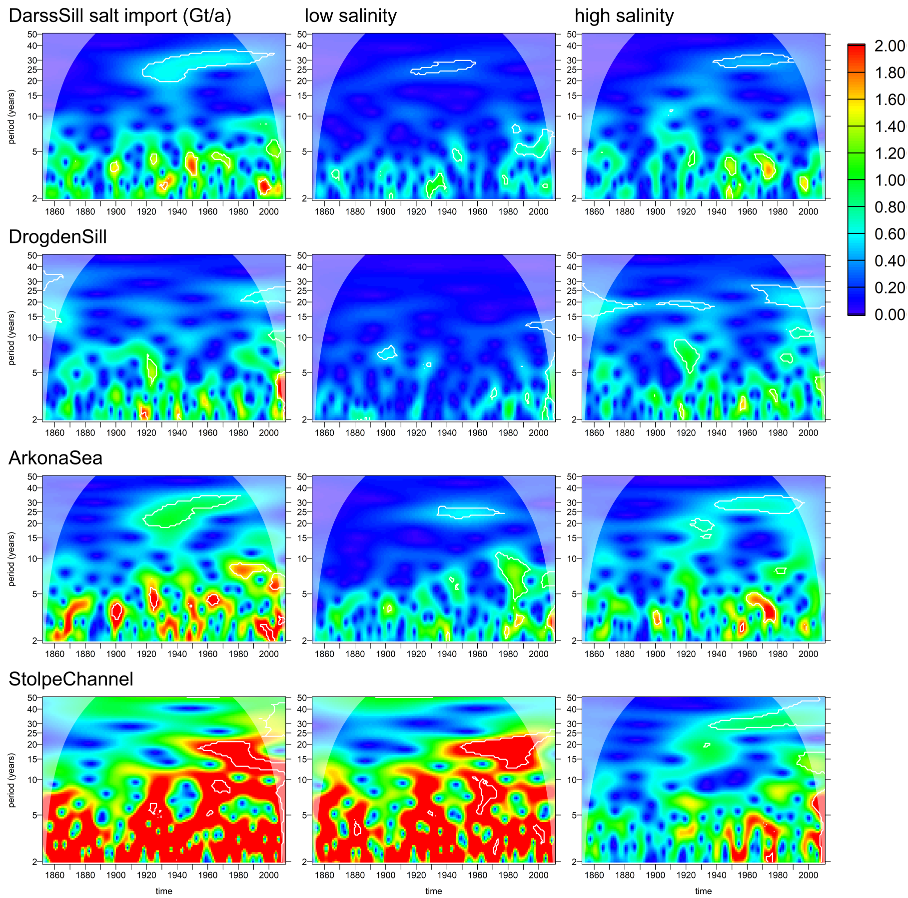

Figure 12. Wavelet amplitudes of net salt import across selected transects. Left column: $T_{\hat{S},t}$ (transport in all salinities above $\hat{S}$). Middle column: $T_{lowsal,t}$ (salinities above $\hat{S}$ but below $S_{in}^{50\%}$) Right column: $T_{highsal,t}$ (salinities above $S_{in}^{50\%}$)

above the threshold salinity where typically import equals export, $T_{\hat{S},t}$ as well the subdivision into the lower and upper salinity range, $T_{lowsal,t}$ and $T_{highsal,t}$.

We find significant wavelet power in the DarssSill import at the 30-year frequency band from 1920 on. Both low and high salinities contribute to this variation. The Drogden Sill import, in contrast, does not show a 30-year variation, the dominating interdecadal variations occur at lower periods around 20 years here.

The import across the ArkonaSea transect [1] shows similar patterns to the DarssSill variations, but the signal increases in magnitude, reflecting an increase of the total volume transport due to entrainment. Transports across Stolpe Channel vary by more than 2 $\mathrm{Gt\,a^{-1}}$ at lower salinities at different periods up to 20 years. The import at higher salinities (above 11.15 $\mathrm{g\,kg^{-1}}$),

[1] For the DarssSill transect, the image looks almost identical to Fig. 13 (not shown).

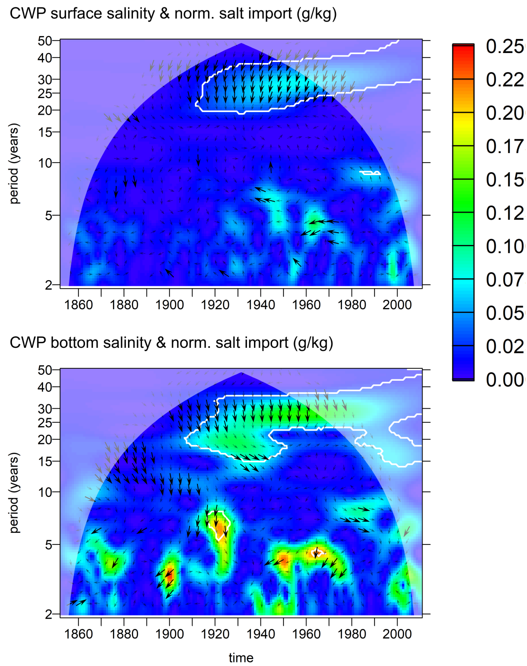

Figure 13. Common wavelet power between modelled surface and bottom salinity at station BY15 (Eastern Gotland Basin) and the normalised time series of $T_{\hat{S},t}$ across the transect ArkonaSea ($\mathrm{g\,kg^{-1}}$). White contours indicate that the WA/CWP is significant at the 95% confidence level with respect to a random shuffling of the annual means of the salt import. Arrows indicate relative phase: →=in phase, ↓=salt import leading salinity by 90°. Thick arrows indicate phase stability (wavelet coherence > 0.95).

however, shows a similar signal as the import across ArkonaSea in total, with significant energy in the 30-year frequency band from 1930 onwards.

Fig. 13 shows the common wavelet power between the normalised salt import $T_{\hat{S},t}$ across the ArkonaSea transect and the surface or bottom salinity at station BY15 in the numerical model. We see that significant common wavelet power exists in the 30-year frequency band from around 1910 on both for surface and bottom salinities. We can see that the common wavelet power between salt import and bottom salinities is about twice as large compared to surface salinities. This is in line with the empirical results shown in Fig. 11. Wavelet coherence above 0.95 exists in the 30-year frequency band. Here, the salt import is leading bottom salinities by 60–90°, which means 5–7.5 years, and the surface salinities by more than 90°, which means a time lag around 8 years. For variations with shorter periods up to 10 years, common wavelet power occurs intermittently but is hardly ever statistically significant. The phase relation, however, shows that in cases where phase stability exists, salt import is always leading bottom salinity, however, at differing lag times. In relation to surface salinity, we find phase lags between 135 and 225°, indicating that larger salt imports occur during periods of low surface salinity if time scales below 10 years are considered.

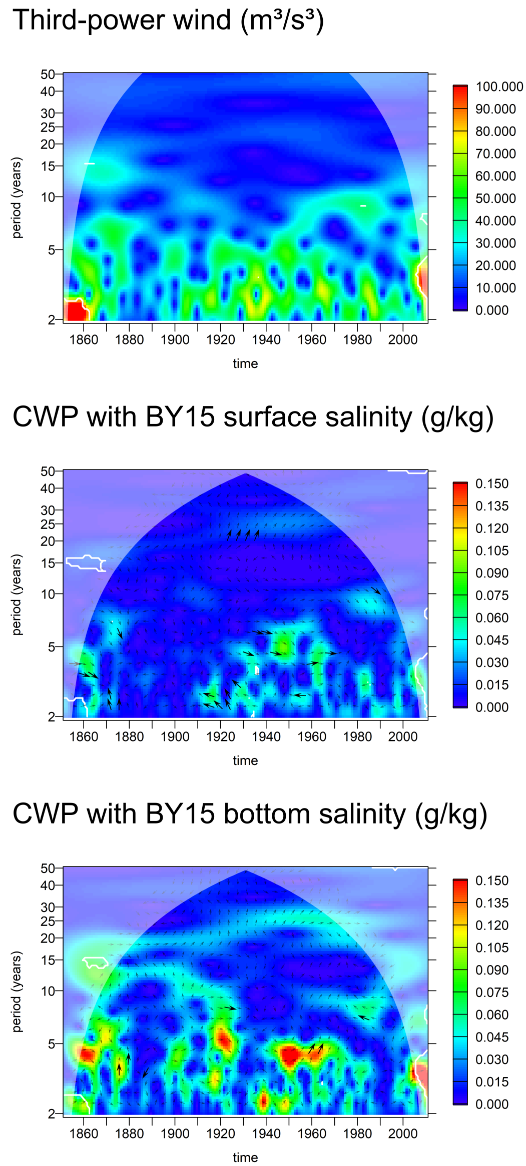

Figure 14. Top row: Wavelet amplitude of the third power of the wind speed ($\mathrm{m}^3\ \mathrm{s}^{-3}$). Middle row: Common wavelet power between modelled surface salinity and normalised third-power wind ($\mathrm{g\,kg}^{-1}$). Bottom row: The same for bottom salinity. All variables at station BY15 (Eastern Gotland Basin). White contours indicate that the WA/CWP is significant at the 95% confidence level with respect to a random shuffling of the annual means of the third-power wind. Arrows indicate relative phase: $\rightarrow$=in phase, $\downarrow$=third-power wind leading salinity by 90°. Thick arrows indicate phase stability (wavelet coherence > 0.95).

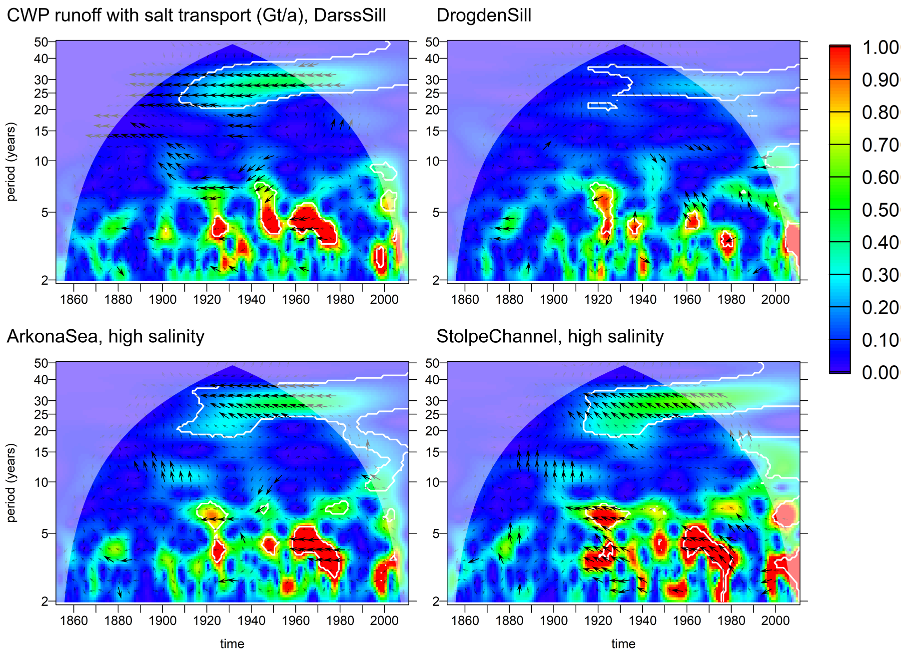

Figure 15. Common wavelet power between salt import across selected transects and normalised annual runoff into the Baltic Sea. $T_{\hat{S},t}$ is chosen as time series for salt import across DarssSill and DrogdenSill transects, while $T_{highsal,t}$ is chosen across ArkonaSea and StolpeChannel. White contours indicate that the WA/CWP is significant at the 95% confidence level with respect to a random shuffling of the annual means of the runoff. Arrows indicate relative phase: →=in phase, ↓=runoff leading salt import by 90°. Thick arrows indicate phase stability (wavelet coherence > 0.95).

4.3.4 Vertical turbulent mixing

We use the third power of the 10-m wind speed as a proxy for interannual variations in the turbulent kinetic energy production which causes vertical mixing. Fig.14 shows the wavelet analysis of the third-power wind at Gotland Deep and its relation to the modelled surface and bottom salinities. Practically no energy exists at the 30-year period. Common energy between third-power wind and salinities is never significant at the 95% confidence level. For surface salinity, however, the relative phase shift between wavelets with common energy is always less than $\pm 90°$ as long as the period is 4 years or longer. This indicates that on these time scales, high surface salinities coincide with strong wind speeds.

4.4 Coherence between runoff and salt import

Finally, we investigate the common wavelet power between net salt import across the sills and the runoff into the Baltic Sea. As we see in Fig. 15, the common wavelet power between the salt import and the normalised runoff is on the order of $0.5\ \mathrm{Gt\,a^{-1}}$ for the DarssSill transect on the 30-year time scale. It is substantially lower for Drogden Sill. At the ArkonaSea and StolpeChannel transects, we especially find high common wavelet power if we consider the transports in the high-salinity range only, here we find a similar common variation around 0.5 $\mathrm{Gt\,a^{-1}}$. Phase stability is very high in the 30-year frequency band, with higher imports across DarssSill taking place during periods of low runoff. At ArkonaSea and StolpeChannel, the salt import slightly lags the lower runoff by about 2 years. If we consider higher frequencies, we intermittently find common wavelet power, partly exceeding 1 $\mathrm{Gt\,a^{-1}}$ and in several cases statistically significant. The phase relation, where it is stable, always shows an opposite-phase component, indicating that the coincidence between low runoff and high salt import is not restricted to the 30-year frequency band.

5 Discussion

5.1 Decadal salinity variations in the Baltic Sea

Wavelet analysis showed that the most relevant time scale on which salinity variations occur in the Central Baltic Sea is the 30-year period. Only for this period, permanent significant wavelet power was found, both in the observations and in the model (Fig. 6–7). In the Western Baltic Sea (Stations BY2 and BY5), interannual variations are stronger anyway but also occur on more variable temporal scales. Observations and model agree quite well in terms of the interannual variations if we visually compare the spectral distributions in Fig. 6 and 7.

In the model, the 30-year oscillation starts to become significant in the first half of the 20th century only, the exact decade depends on the station. Since the observation data start later, we cannot say whether the absence of the oscillations in the 19th century is real or a model artefact. We would like to stress that the wavelet analysis results in the cone of influence should not be interpreted.

We see ~~two~~ three possible reasons why the model could have missed salinity variations in the 19th century: Firstly, the model may have required a spin-up period from its initialisation in 1850 with possibly inconsistent initial conditions. Secondly, the river forcing dataset is not homogenous in time, for 1850–1900 a statistical model was used which was based on atmospheric pressure over land Hansson et al. (2011). Fig. 4 in their study already indicates that the 30-year variability in the runoff may be underestimated by the statistical model. Finally, the atmospheric forcing dataset may show poorer realism further back in the past. The analog method used to create it requires that for each day in the past climate, there is a matching day in the recent reference period whose values are chosen. The mismatch could be larger if past climate and reference climate differ more strongly, leading to a possibly too poor representation of Major Baltic Inflow dynamics.

5.2 Drivers of the variations

5.2.1 Climate indices

The comparison with the climate indices shows that neither NAO nor AMO contain the 30-year signal which is apparent in the Baltic Sea salinity throughout the 20th century. Their dominating time scales are substantially different (below 10 years for NAO, above 60 years for AMO), but also the energy they contain at different periods does not match the 30-year period we are interested in, as the change in relative phase over time shows. The NAO index shows some variation on periods around 35 years, while the AMO has energy at 20–25 years.

These frequency differences to the 30-year period are too large to allow for salinity changes being driven by these indices directly. More accurately phrased, the variability over the North Atlantic which is measured by these indices is most certainly not the driver of the salinity changes throughout the considered period. However, one might speculate that the difference is small enough to have an oscillator with an intrinsic 1/30-year eigenfrequency excited by these external variations, which then continues to oscillate after the initial forcing ended. So, we cannot rule out that the climate indices play an indirect role for the salinity variations.

5.2.2 Influence of vertical turbulent mixing

As Fig. 14 shows, there is almost no variation of third-power wind at station BY15 with a period around 30 years, so a variation in the generation of turbulent kinetic energy and a corresponding change in the vertical mixing across the halocline can be ruled out as driver of the interdecadal salinity changes.

5.2.3 Runoff and salt import

River runoff and surface salinity show a very similar pattern in their wavelet decomposition at multi-decadal time scales (compare Fig. 9 with Fig. 6). Interdecadal salinity variations in the model start at the beginning of the 20th century, which is when they also start in the river forcing. The phase relationship is as expected, periods of low salinity follow those of increased river runoff, at least in the interdecadal variability. What is counterintuitive is that the covariations of the bottom salinity with runoff (a) are stronger than at the surface and (b) are slightly leading the variations in surface salinity (Fig. 9).

The relationship between Baltic Sea salinity and salt import was studied by two different approaches in Fig. 11 and Fig. 13: By relating observed salinity changes to the barotropic inflow reconstruction of Mohrholz (2018), and by relating modelled salinity changes to the net salt import above a specific salinity threshold in the model. Since the amount of salt in the Baltic Sea is exactly determined by the salt transports in and out, we should expect the 30-year period from the salinity fluctuations to also occur in the salt import; both methods confirm this thought (Fig. 10 and Fig. 12). The phase lag between high salt import and high bottom salinities is around 60° (somewhat larger in the model), between salt import and surface salinities we find approximately 90° phase difference. This means that bottom salinity changes slightly before surface salinity. The fact that it also shows stronger variations than surface salinity indicates that salinity oscillations below the halocline drive those above the halocline, not vice versa as would be expected if the salinity changes were directly controlled by runoff.

The results are in excellent agreement with Meier and Kauker (2003b). They found in a similar model study that the cumulated runoff anomaly excellently explained the decadal changes in mean salinity. However, an additional sensitivity simulation with identical runoff in each year still reproduced the stagnation periods of the 1920s and 1980s. This proves that a driver different from runoff explains part of the decadal variability in salinity. Meier and Kauker (2003b) showed that enhanced zonal wind over the Baltic Sea during stagnation periods both increases precipitation in the catchment and reduces inflow activity. This link between runoff and inflow activity, however, can only explain a part of the decadal variability in salinity. Wavelet analysis of the zonal wind component at the Swedish meteorological station Landsort (SMHI, 2019) indicates that interdecadal variations are prominent on the 20-year rather than the 30-year time scale.

Since the strong westerly winds are the result of favourably aligned storm tracks, barotropic inflows are considered rather random and unpredictable, so it is not obvious why they show a 30-year variation in their total salt import. Fig. 10 shows that it is not the total frequency of the inflow events that changes, but the average amount of salt which an individual inflow event transports into the Baltic Sea. This causes the frequency of strong inflows (DS5 events) to change significantly, and correspondingly the total salt flux.

So, both river runoff and the strength of barotropic inflow events show a variation on the 30-year time scale, and both of them show a stable and plausible phase relationship to be the drivers of the interdecadal salinity fluctuations. This means that from correlation analysis alone, we cannot tell which of the processes is responsible for which fraction of the salinity change. Asked differently, are interdecadal variations in wind patterns or in precipitation over land responsible for the observed salinity oscillations? This is especially important if the negative covariance between inflow intensity and river runoff was by coincidence in the past and will not continue into the future. Fig. 15 shows this very clear opposite phase relationship between river runoff and salt import across the DarssSill transect (top left subfigure), but it is not yet known whether a deterministic physical mechanism links the two on the 30-year time scale. The existence of two synchronous mechanisms causing salinity changes in the Baltic Sea complicates the validation of circulation models applied for future climate projections. Verifying that a model was able to capture the multidecadal climate variations in the historical period might not be sufficient to prove that its sensitivity of salinity towards changes in runoff is realistic. Instead, a model could e.g. overestimate the sensitivity of salinity to runoff and underestimate that to changes in wind, or vice versa. For climate projections on Baltic Sea freshening, this means an additional source of uncertainty.

The major findings from the wavelet coherence analysis are summarized in Table 2.

6 Estimation of the direct dilution effect

We can think of at least four pathways in which Baltic Sea salinity would vary at the same frequency as the runoff:

- Direct dilution effect: The Baltic Sea loses salt due to an enhanced outflow volume caused by increased runoff and net precipitation (Schott, 1966).

- Indirect dilution effect: Higher volume and lower salinity of the Baltic outflow due to enhanced river runoff reduces the salinity of inflowing water, e.g., by increased entrainment into the Kattegat deep water (Rodhe and Winsor, 2002) or a northward shift of the salinity front in the Kattegat.

- Wind patterns systematically linked to runoff: Wind patterns which modify inflow strength could be driven or favoured by the same atmospheric patterns that control the precipitation in the catchment. These variations in salt import could therefore be systematically linked to the river runoff, although not being a consequence of it.

Table 2. Summary of the findings of the wavelet coherence analysis

First time series BY15 modelled salinity at	Second time series	Significant CWP (time range, period)	Phase lag
surface or bottom	NAO	-	-
surface or bottom	AMO	1920-1970, 20-25 years	unstable
surface	negative runoff anomaly	1920-1980[a], 25-30 years	salinity lagging by 90°
bottom	negative runoff anomaly	1920-1980[a], 25-30 years	salinity lagging by <90°
surface	Salt import across Darss Sill (Mohrholz 2018)	1940[a]-1980[a], 30 years	salinity lagging by 90°
bottom	Salt import across Darss Sill (Mohrholz 2018)	1940[a]-1980[a], 30 years	salinity lagging by <90°
surface	Salt import across Arkona Sea transect, modelled	1910-1980[a], 25-30 years	salinity lagging by 90°
bottom	Salt import across Arkona Sea transect, modelled	1910-1980[a], 25-30 years	salinity lagging by <90°
surface or bottom	third power of wind at BY15	-	-

[a] Possibly outside this range, since this date is the cone of influence

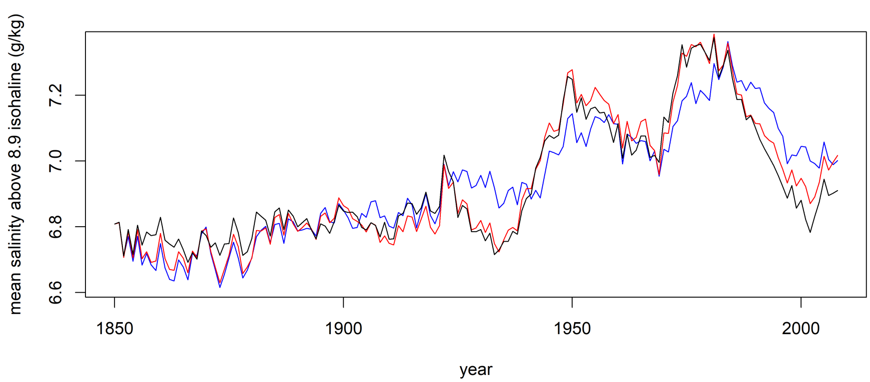

Figure 16. Fig. 16: Baltic Sea annual mean salinity above the 8.9 $\mathrm{g\,kg^{-1}}$ isohaline ($\mathrm{g\,kg^{-1}}$). Black: Results of numerical model. Red: After the approximation that the outflow salinity is the mean salinity modified by a factor α. Blue: Additionally under the assumption of a constant river runoff.

– Wind patterns only coincidentally linked to runoff: The link between strong inflows and low river runoff could be just coincidental during the instrumental period.

To estimate the direct dilution effect, we apply the salt budget calculations described in Section 2.5. The mean salinity in the Baltic Sea above the isohaline of 8.9 $\mathrm{g\,kg^{-1}}$, which is the value of $\hat{S}$ for the ArkonaSea transect, is shown in Fig. 16 for three different models: The full numerical model, the same simplified by the assuming a constant ratio α between mean salinity and outflowing salinity, and the model assuming both constant α and constant runoff. We find that assuming a constant α does not have a large effect on the mean salinity in the upper layer. The assumption of a constant river runoff, in contrast, has an impact on surface salinity: It reduces the standard deviation of salinity by 10.6% for the complete time series, or by 27.2% if we consider the period from 1910 only where we find the 30-year oscillations. So, we can estimate that the direct dilution effect is responsible for about one fourth of the salinity variations in this period. This may be a lower estimate, since the GETM model overestimates surface salinities in general and may therefore underestimate the influence of river water on the surface layer.

7 Conclusions and outlook

7.1 Conclusions

A ~~realistic~~ 159-year hindcast simulation was conducted using the GETM model to understand interdecadal variations in Baltic Sea salinity. Even though the model results show a positive bias in mean salinities which increases from south to north, the interdecadal variations in salinity were captured well by the model making it applicable for our study.

A 30-year variability was found in the following quantities:

- Surface and bottom salinities at seven different oceanographic stations, both in the model and in observations
- River runoff into the Baltic Sea
- Salt transports across Darss Sill, especially during inflow events which last for at least five days

No such variability was found in third-power wind speeds or in the climate indices NAO or AMO.

Runoff is one of the drivers of multidecadal variability of Baltic Sea salinity, but the direct dilution effect was found to be responsible for about one fourth of the oscillations only. The impact of vertical turbulent mixing on multidecadal variability is small. Salt water inflows contribute to the multidecadal variability in salinity as well, in particular of the bottom layer salinity.

7.2 Outlook

The total effect of runoff on salinity, the sum of direct and indirect dilution effect, can be determined by sensitivity runs of a numerical model, artificially setting the runoff to constant. Such a sensitivity experiment with climatological river runoff, but realistic wind forcing, has been conducted by Meier and Kauker (2003b), and interdecadal salinity variations were reduced by about half (Scenario F1 in their Fig. 11). This suggests that if the models agree, both direct and indirect effect of river runoff could explain about 50% of the salinity changes. To find out whether this number (25% for indirect effect of river runoff) is realistic or a model artefact, one would need to check whether the processes that propagate the outflow water signal to the inflow strength are correctly represented. We will do so in ongoing sensitivity experiments. To identify and quantify these physical mechanisms in model simulations and then verify them in field studies would be an important next step to estimate the vulnerability of Baltic Sea salinity to runoff changes. For example, if entrainment of Baltic outflow water into the Kattegat deep water is identified as a major process in the model, the turbulence ~~parameterisation~~ parameterization would be critical for realistically estimating this mixing intensity. The discrimination between the wind and runoff effect might, however, be impossible if non-linear interactions between the two play a significant role, such that their combined effect is different from the sum of both effects individually.

Another important question is whether the wind-driven changes in inflow strength (according to the study of Meier and Kauker (2003b) the remaining 50% together with inflow frequency) are intrinsically related to changes in runoff. That is, can an atmospheric pattern be identified which at the same time increases precipitation in the Baltic Sea catchment and decreases inflow strength?

The identification of a climate pattern which controls precipitation over the Baltic Sea catchment on a decadal time scale should be of importance not only for ocean science. If an oscillator exists in nature which shows an intrinsic period of 30 years and affects river runoff, its identification would allow predicting trends in river runoff over lead times of a decade. If the present amplitude and phase of the oscillatory pattern could be detected, this decadal lead time would e.g. allow to initiate engineering measures for river flood protection.

Code and data availability. TEXT

The GETM model used for this study is open-source software and can be downloaded from https://getm.eu/. The data we used can be obtained from their respective sources mentioned in Section 2.1. The time series we analysed are available on request from the corresponding author.

Appendix A: Coordinates of oceanographic stations

Locations of oceanographic stations and borders of the corresponding boxes for selecting ICES observations are given in Table A1.

Appendix B: Salinity thresholds for the transects

Salinity thresholds for the transects are given in Table B1.

Appendix C: Details on model setup

Three sub-grid-scale parameterisations are applied in the model:

– Firstly, turbulent vertical diffusivity and viscosity are calculated by the General Ocean Turbulence Model (GOTM, www.gotm.net). A second-order Mellor-Yamada model is used (Mellor and Yamada, 1982; Umlauf and Burchard, 2005),

Table A1. Locations of oceanographic stations and borders of the corresponding boxes for selecting ICES observations (°N or °E).

station	latitude	longitude	lat_north	lat_south	lon_west	lon_east
BY2	55.000	14.083	55.2	54.8	13.2	14.2
BY5	55.250	15.983	55.6	54.9	15.3	16.2
BMPL1	54.833	19.333	55.2	54.5	18.8	19.7
BY15	57.333	20.050	57.5	56.8	19.5	20.5
OMTF0286	58.000	19.900	58.3	57.8	19.5	20.2
BY31	58.583	18.233	58.8	58.2	18.1	19.0
F64	60.189	19.143	60.3	59.8	18.8	19.8

Table B1. Modelled salinity thresholds for selected transects ($\mathrm{g\,kg^{-1}}$)

station	$\hat{S}$	$S_{in}^{50\%}$
ArkonaSea	8.90	13.45
DarssSill	11.15	15.20
DrogdenSill	11.60	19.68
GreatBelt	18.72	24.18
LittleBelt	20.35	23.15
StolpeChannel	7.25	11.15

which solves dynamic equations for turbulent kinetic energy (TKE, k) and a turbulence length scale L. To derive vertical mixing efficiencies from these, we use coefficients given by Canuto et al. (2001).

- Secondly, turbulent horizontal diffusivity and viscosity are prescribed by a Smagorinsky scheme (Smagorinsky, 1963). Since the model uses terrain-following coordinates, the Smagorinsky mixing is not strictly horizontal but contains a vertical component especially at sloping topography. So, this numerical scheme can also be used to parametrise boundary mixing, which is the major component for vertical diffusion in the deep areas of the central Baltic Sea (Holtermann et al., 2012). To account for this, we set the Prandtl number for the turbulent horizontal exchange to 4.

- Finally, we parameterise the effect of Langmuir circulation (Langmuir, 1938) on vertical mixing. The approach follows Axell (2002): Langmuir circulations are included as an additional production term for TKE. Its input is proportional to the third power of the 10-m wind speed.

The model includes a thermodynamic sea ice model (Winton, 2000), but no dynamic component, i.e. ice drift and especially the increase of ice thickness due to drift-induced ridging and rafting (Mårtensson et al., 2012) is not explicitly represented. Since this implies that the model would underestimate ice thicknesses and the ice-covered period, we introduce empirical correction factors to the freezing and melting processes. While ice growth is accelerated by a factor of 1.9, the melting of ice is decelerated by the same factor. This also accounts for the unresolved ice-ocean boundary layer.

Measurements of ocean temperature and salinity are scarce in the 19th century and, to the best of our knowledge, completely lacking in the Baltic Sea for the first model year, 1850. As a result, defining initial conditions for the model is not straightforward. We use measurements from the year 1979 and extrapolate them to the model grid. This rather arbitrary choice obviously induces a substantial amount of uncertainty, especially for the first decades. However, the unavoidable deviations from the unknown reality can be expected to decrease over a time scale of about 30–40 years, which is the typical time scale in which Baltic Sea water is renewed by inflows from the Kattegat (Meier, 2007).

Appendix D: Details on wavelet analysis

For the dimensionless shape parameter in the Morlet wavelet, we choose a standard value of $\omega_0 = 6$ as suggested by Grinsted et al. (2004), so the oscillatory term in equation (9) has a period of $T = 2\pi a/6 \approx 1.05a$ ~~.~~ (Fig. D1). The scaling factor in equation (9) is chosen in such a way that the wavelet transform of any of the two functions

$$f_1(t) = b sin(2\pi t/T), \qquad f_2(t) = b cos(2\pi t/T) \tag{D1}$$

gives a wavelet amplitude $|W(a,t)|$ equal to b, see the proof in the online supplement. The wavelet transform measures the correlation between the signal and the wavelet. A value of $W(a,t) = b$ means that the analysed time series shows the same correlation with the wavelet as a harmonic function with amplitude b. A value different from zero does not necessarily mean that a periodic signal was detected at time t, it just means the signal shows some similarity to the wavelet. Since the wavelet is complex, $Re(b)$ describes the correlation with the real part of ϕ and $Im(b)$ describes the correlation with the negative imaginary part of ϕ, so $arg(b)$ contains the phase information. When we perform wavelet transforms of ICES observation data, we use the ~~deseasonalised~~ deseasonalized annual means and fill the gaps in the time series by linear interpolation.

To check whether wavelet amplitude (WA) or common wavelet power (CWP) are significant, we generate an ensemble of randomized time series, created by shuffling the years of the original time series. For CWP, we only shuffle the second (the explanatory) time series. Then we calculate the time average of the 95th percentile of the randomized WA or CWP, giving a critical value for each frequency. Where the signal exceeds this threshold, it is considered as significant.

Wavelet coherence is calculated as

$$\rho_{xy}(a,t) \quad = \quad \frac{< W_x(a',t') W_y * (a',t') >}{\sqrt{< |W_x(a',t')|^2 >< |W_y(a',t')|^2 >}} \tag{D2}$$

(Aguiar-Conraria and Soares, 2011), where the pointed brackets mean a smoothing over a time and frequency range around the central point (a,t). In the simplest case this can be a box average over a time and frequency interval. In case that the relative phase is equal throughout this range, it can be factored out from the averaging operator in the numerator, so ρ_{xy} has a magnitude of one then. If, in contrast, the relative phase varies strongly across the averaging interval, the magnitude of ρ_{xy} will

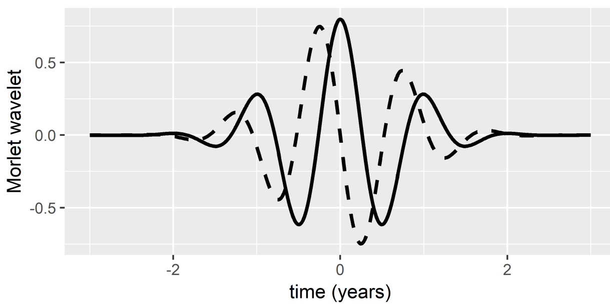

Figure D1. The Morlet wavelet for the temporal scale $a = 1$ year and $\omega_0 = 6$. Solid line: real part. Dashed line: imaginary part. Please note that the periodicity almost matches the temporal scale.

615 be close to zero. We choose a simple box average over the intervals $t \in [t-a, t+a]$ and $a \in [a-a/8, a+a/8]$ as the smoothing operator in equation (D2).

Appendix E: Discussion about the differences between stations in explained variance of the bottom salinity time series

Baltic Sea bottom salinity is controlled by inflowing water from the North Sea. This water passes a series of sills under favourable meteorological conditions and is diluted on its pathway by the intrusion of ambient water. One might therefore expect that the mismatch between reality and model in the bottom salinity increases with increasing distance to the North Sea, since errors accumulate across this path.

The explained variance on decadal scale (see Table 1) shows the opposite: It decreases from Arkona Sea (BY2, 13%) to Bornholm Sea (BY5, -56%) but increases again in the Central Baltic to reach its maximum value (BY15, 52%). The negative explained variance at BY5 even means that model and observations show a negative correlation in the decadal time series.

One possible explanation for this paradox is that it is not the bottom salinity in one basin that controls the salt inflow into the next one, but rather the salinity at the sill depth. If we consider salinity at 60 m depth at station BY5, we actually get a positive value for explained variance of 22% (interdecadal) and 34% (interannual), which shows that only the salinity in the very deepest part of the Bornholm Basin (93 m deep) shows an opposite interdecadal trend in the model.

The fact that the interdecadal variation is still captured best in the Eastern Gotland Basin might indicate that the volume transports are actually more important than the salinities for determining the salt flux into the basin. During single inflow events, it is crucial that the salinity of an inflowing plume is high enough to change the bottom salinity. On a decadal scale, also less dense inflows that show interleaving (reach a depth below the halocline but not the deepest part of the basin) may change the bottom salinity indirectly by reducing vertical upward diffusion of salt.

Another possible explanation is that processes inside the Baltic Sea effectively control its decadal bottom salinity, such that the inflow process plays a less important role on these time scales. It remains speculative which processes can play this role, but mixing processes controlling the halocline strength could plausibly influence bottom salinity. While we showed that the third power of the wind as a proxy for the direct wind work does not show energy in the frequency band of interest, a variation of e.g. upwelling intensity and correspondingly mesoscale activity could represent such a local control mechanism. Identifying such possible local influences on bottom salinity will require more detailed investigations.

Author contributions. HR performed the model simulations and did the analyses. SEB prepared boundary data for the model. UG created the model setup. HEMM supervised the work. All authors contributed to the discussion of the results and to the manuscript.

Competing interests. No competing interests are present for any of the authors.

Acknowledgements. The research presented in this study is part of the Baltic Earth program (Earth SystemScience for the Baltic Sea region, see https://www.baltic.earth). Observations from the long-term, environmental monitoring program at IOW have been used and are publicly available from http://iowmeta.io-warnemuende.de. Model calculations were performed at the supercomputing center of the Norddeutscher Verbund für Hoch- und Höchstleistungsrechnen (HLRN). Data processing was carried out on servers funded by the BMBF projekt PROSO, grant number 03F0779A. Free software which supported this work includes R, R Studio, cdo and ferret.

References

Aguiar-Conraria, L. and Soares, M. J.: The continuous wavelet transform: A primer, Tech. Rep. 16, Núcleo de Investigação em Políticas Económicas, Universidade do Minho, Minho, Portugal, https://repositorium.sdum.uminho.pt/bitstream/1822/12398/4/NIPE_WP_16_2011.pdf, 2011.

Axell, L. B.: Wind-driven internal waves and Langmuir circulations in a numerical ocean model of the southern Baltic Sea, Journal of Geophysical Research: Oceans, 107, 2002.

Bergström, S. and Carlsson, B.: River runoff to the Baltic Sea - 1950-1990, Ambio, 23, 280–287, 1994.

Burchard, H., Bolding, K., Feistel, R., Gräwe, U., Klingbeil, K., MacCready, P., Mohrholz, V., Umlauf, L., and van der Lee, E. M.: The Knudsen theorem and the Total Exchange Flow analysis framework applied to the Baltic Sea, Progress in oceanography, 165, 268–286, 2018.

Canuto, V. M., Howard, A., Cheng, Y., and Dubovikov, M. S.: Ocean turbulence. Part I: One-point closure model—Momentum and heat vertical diffusivities, Journal of Physical Oceanography, 31, 1413–1426, 2001.

Cyberski, J., Wróblewski, A., and Stewart, J.: Riverine water inflows and the Baltic Sea water volume 1901-1990, Hydrology and Earth System Sciences, 4, 1–11, https://doi.org/https://doi.org/10.5194/hess-4-1-2000, https://www.hydrol-earth-syst-sci.net/4/1/2000/hess-4-1-2000.html, 2000.

Gailiušis, B., Kriaučiūnienė, J., Jakimavičius, D., and Šarauskienė, D.: The variability of long–term runoff series in the Baltic Sea drainage basin, Baltica, 24, 45–54, 2011.

Good, R. and Fletcher, H. J.: Reporting explained variance, Journal of Research in Science Teaching, 18, 1–7, publisher: Wiley Online Library, 1981.

Graham, P.: Modeling runoff to the Baltic Sea, Ambio, 28, 328–334, 1999.

Grinsted, A., Moore, J. C., and Jevrejeva, S.: Application of the cross wavelet transform and wavelet coherence to geophysical time series, Nonlinear processes in geophysics, 11, 561–566, 2004.

Gräwe, U., Klingbeil, K., Kelln, J., and Dangendorf, S.: Decomposing mean sea level rise in a semi-enclosed basin, the Baltic Sea, Journal of Climate, 2019.

Gustafsson, B. G. and Andersson, H. C.: Modeling the exchange of the Baltic Sea from the meridional atmospheric pressure difference across the North Sea, Journal of Geophysical Research: Oceans, 106, 19 731–19 744, https://doi.org/10.1029/2000JC000593, https://agupubs.onlinelibrary.wiley.com/doi/abs/10.1029/2000JC000593, _eprint: https://agupubs.onlinelibrary.wiley.com/doi/pdf/10.1029/2000JC000593, 2001.

Gustafsson, B. G., Schenk, F., Blenckner, T., Eilola, K., Meier, H. M., Müller-Karulis, B., Neumann, T., Ruoho-Airola, T., Savchuk, O. P., and Zorita, E.: Reconstructing the development of Baltic Sea eutrophication 1850–2006, Ambio, 41, 534–548, 2012.

Hansson, D., Eriksson, C., Omstedt, A., and Chen, D.: Reconstruction of river runoff to the Baltic Sea, AD 1500–1995, International Journal of Climatology, 31, 696–703, 2011.

Höflich, K., Lehmann, A., and Myrberg, K.: Towards an improved mechanistic understanding of major saltwater inflows into the Baltic Sea, https://doi.org/10.5281/zenodo.3567086, https://zenodo.org/record/3567086#.XnOWwHJCdPY, library Catalog: Zenodo, 2017.

Höflich, K., Lehmann, A., and Myrberg, K.: Decadal variations in barotropic inflow characteristics and their relation with Baltic Sea salinity variability, https://doi.org/10.5281/zenodo.3567070, https://zenodo.org/record/3567070#.XnOfRHJCdPY, library Catalog: Zenodo, 2018.

Höglund, A., Meier, H. E. M., Broman, B., and Kriezi, E.: Validation and correction of regionalised ERA-40 wind fields over the Baltic Sea using the Rossby Centre Atmosphere model RCA3.0, Tech. Rep. 97, SMHI, Norrköping, 2009.

Häkansson, B. G., Broman, B., and Dahlin, H.: The flow of water and salt in the Sound during the Baltic Major Inflow event in January 1993, Tech. Rep. 1993/C:58, ICES, Copenhagen, http://www.ices.dk/sites/pub/CM%20Doccuments/1993/C/1993_C58.pdf, 1993.

Holtermann, P. L., Umlauf, L., Tanhua, T., Schmale, O., Rehder, G., and Waniek, J. J.: The Baltic Sea tracer release experiment: 1. Mixing rates, Journal of Geophysical Research: Oceans, 117, 2012.

ICES: ICES Oceanography, https://ocean.ices.dk/HydChem/HydChem.aspx?plot=yes, 2019.

Jones, P. D., Jonsson, T., and Wheeler, D.: Extension to the North Atlantic oscillation using early instrumental pressure observations from Gibraltar and south-west Iceland, International Journal of Climatology, 17, 1433–1450, https://doi.org/10.1002/(SICI)1097-0088(19971115)17:13<1433::AID-JOC203>3.0.CO;2-P, https://rmets.onlinelibrary.wiley.com/doi/abs/10.1002/%28SICI%291097-0088%2819971115%2917%3A13%3C1433%3A%3AAID-JOC203%3E3.0.CO%3B2-P, 1997.

Kennedy, J. J., Rayner, N. A., Smith, R. O., Parker, D. E., and Saunby, M.: Reassessing biases and other uncertainties in sea surface temperature observations measured in situ since 1850: 1. Measurement and sampling uncertainties, Journal of Geophysical Research, 116, https://doi.org/10.1029/2010JD015218, http://doi.wiley.com/10.1029/2010JD015218, 2011a.

Kennedy, J. J., Rayner, N. A., Smith, R. O., Parker, D. E., and Saunby, M.: Reassessing biases and other uncertainties in sea surface temperature observations measured in situ since 1850: 2. Biases and homogenization, Journal of Geophysical Research, 116, https://doi.org/10.1029/2010JD015220, http://doi.wiley.com/10.1029/2010JD015220, 2011b.

Khlebovich, V. V.: Aspects of animal evolution related to critical salinity and internal state, Marine Biology, 2, 338–345, https://doi.org/10.1007/BF00355713, http://link.springer.com/10.1007/BF00355713, 1969.

Kniebusch, M., Meier, H. E. M., Neumann, T., and Börgel, F.: Temperature Variability of the Baltic Sea Since 1850 and Attribution to Atmospheric Forcing Variables, Journal of Geophysical Research: Oceans, 124, 4168–4187, https://doi.org/10.1029/2018JC013948, https://agupubs.onlinelibrary.wiley.com/doi/abs/10.1029/2018JC013948, 2019.

KNMI: Climate Explorer: Select a monthly time series, https://climexp.knmi.nl/selectindex.cgi?id=someone@somewhere, 2019.

Langmuir, I.: Surface motion of water induced by wind, Science, 87, 119–123, 1938.

Lass, H. U. and Matthäus, W.: On temporal wind variations forcing salt water inflows into the Baltic Sea, Tellus A, 48, 663–671, http://onlinelibrary.wiley.com/doi/10.1034/j.1600-0870.1996.t01-4-00005.x/abstract, 1996.

Mårtensson, S., Meier, H. E. M., Pemberton, P., and Haapala, J.: Ridged sea ice characteristics in the Arctic from a coupled multicategory sea ice model, Journal of Geophysical Research: Oceans, 117, 2012.

MacCready, P.: Calculating Estuarine Exchange Flow Using Isohaline Coordinates, Journal of Physical Oceanography, 41, 1116–1124, https://doi.org/10.1175/2011JPO4517.1, https://journals.ametsoc.org/doi/full/10.1175/2011JPO4517.1, 2011.

MacKenzie, B. R., Gislason, H., Möllmann, C., and Köster, F. W.: Impact of 21st century climate change on the Baltic Sea fish community and fisheries, Global Change Biology, 13, 1348–1367, 2007.

Malmberg, S.-A. and Svansson, A.: Variations in the physical marine environment in relation to climate, Tech. Rep. 1982/Gen:4, International Council for the Exploration of the Sea, Copenhagen, http://www.ices.dk/sites/pub/CM%20Doccuments/1982/Gen/1982_Gen4.pdf, not to be cited without prior reference to the authors!, 1982.

Maraun, D. and Kurths, J.: Cross wavelet analysis: significance testing and pitfalls, Nonlinear Processes in Geophysics, 11, 505–514, 2004.

Meier, H. E. M.: Modeling the pathways and ages of inflowing salt- and freshwater in the Baltic Sea, Estuarine, Coastal and Shelf Science, 74, 610–627, https://doi.org/10.1016/j.ecss.2007.05.019, http://www.sciencedirect.com/science/article/pii/S0272771407001631, 2007.

Meier, H. E. M. and Kauker, F.: Sensitivity of the Baltic Sea salinity to the freshwater supply, Climate Research, 24, 231–242, https://doi.org/10.3354/cr024231, http://www.int-res.com/abstracts/cr/v24/n3/p231-242/, 2003a.

Meier, H. E. M. and Kauker, F.: Modeling decadal variability of the Baltic Sea: 2. Role of freshwater inflow and large-scale atmospheric circulation for salinity, Journal of Geophysical Research: Oceans, 108, 3368, https://doi.org/10.1029/2003JC001799, http://onlinelibrary.wiley.com/doi/10.1029/2003JC001799/abstract, 2003b.

Meier, H. E. M., Eilola, K., Almroth-Rosell, E., Schimanke, S., Kniebusch, M., Höglund, A., Pemberton, P., Liu, Y., Väli, G., and Saraiva, S.: Disentangling the impact of nutrient load and climate changes on Baltic Sea hypoxia and eutrophication since 1850, Climate Dynamics, pp. 1–22, 2018a.

Meier, H. M., Andersson, H. C., Arheimer, B., Blenckner, T., Chubarenko, B., Donnelly, C., Eilola, K., Gustafsson, B. G., Hansson, A., and Havenhand, J.: Comparing reconstructed past variations and future projections of the Baltic Sea ecosystem—first results from multi-model ensemble simulations, Environmental Research Letters, 7, 034 005, 2012.

Meier, H. M., Väli, G., Naumann, M., Eilola, K., and Frauen, C.: Recently accelerated oxygen consumption rates amplify deoxygenation in the Baltic Sea, Journal of Geophysical Research: Oceans, 123, 3227–3240, 2018b.

Mellor, G. L. and Yamada, T.: Development of a turbulence closure model for geophysical fluid problems, Reviews of Geophysics, 20, 851–875, 1982.

Mikulski, Z.: Inflow from drainage basin, in: Water Balance of the Baltic Sea, vol. 16 of *Baltic Sea Environment Proceedings*, pp. 24–34, Baltic Marine Environment Protection Commission, Helsinki, 1986.

Mohrholz, V.: Major Baltic Inflow Statistics – Revised, Frontiers in Marine Science, 5, https://doi.org/10.3389/fmars.2018.00384, https://www.frontiersin.org/article/10.3389/fmars.2018.00384/full, 2018.

Oldenborgh, G. J. v., Raa, L. A. t., Dijkstra, H. A., and Philip, S. Y.: Frequency- or amplitude-dependent effects of the Atlantic meridional overturning on the tropical Pacific Ocean, Ocean Science, 5, 293–301, https://doi.org/https://doi.org/10.5194/os-5-293-2009, https://www.ocean-sci.net/5/293/2009/os-5-293-2009.html, 2009.

Rodhe, J. and Winsor, P.: On the influence of the freshwater supply on the Baltic Sea mean salinity, Tellus A, 54, 175–186, https://doi.org/10.1034/j.1600-0870.2002.01307.x, http://tellusa.net/index.php/tellusa/article/view/12134, 2002.

Rodhe, J. and Winsor, P.: On the influence of the freshwater supply on the Baltic Sea mean salinity, Tellus A, 55, 455–456, https://doi.org/10.1034/j.1600-0870.2003.00037.x, http://tellusa.net/index.php/tellusa/article/view/12112, 2003.

Schenk, F. and Zorita, E.: Reconstruction of high resolution atmospheric fields for Northern Europe using analog-upscaling, Climate of the Past, 8, 1681, 2012.

Schimanke, S. and Meier, H. E. M.: Decadal-to-Centennial Variability of Salinity in the Baltic Sea, Journal of Climate, 29, 7173–7188, https://doi.org/10.1175/JCLI-D-15-0443.1, https://journals.ametsoc.org/doi/full/10.1175/JCLI-D-15-0443.1, publisher: American Meteorological Society, 2016.

Schott, F.: Der Oberflächensalzgehalt in der Nordsee, Deutsche Hydrografische Zeitschrift, p. 58, 1966.

Seifert, T., Tauber, F., and Kayser, B.: A high resolution spherical grid topography of the Baltic Sea – 2nd edition, https://www.io-warnemuende.de/topography-of-the-baltic-sea.html, 2001.

Smagorinsky, J.: General circulation experiments with the primitive equations: I. The basic experiment, Monthly weather review, 91, 99–164, 1963.

SMHI: Ladda ner meteorologiska observationer, https://www.smhi.se/data/meteorologi/ladda-ner-meteorologiska-observationer/#param=airtemperatureInstant,stations=all, 2019.

Umlauf, L. and Burchard, H.: Second-order turbulence closure models for geophysical boundary layers. A review of recent work, Continental Shelf Research, 25, 795–827, 2005.

Vuorinen, I., Hänninen, J., Rajasilta, M., Laine, P., Eklund, J., Montesino-Pouzols, F., Corona, F., Junker, K., Meier, H. M., and Dippner, J. W.: Scenario simulations of future salinity and ecological consequences in the Baltic Sea and adjacent North Sea areas–implications for environmental monitoring, Ecological indicators, 50, 196–205, 2015.

Walin, G.: A theoretical framework for the description of estuaries, Tellus, 29, 128–136, 1977.

Walin, G.: On the relation between sea-surface heat flow and thermal circulation in the ocean, Tellus, 34, 187–195, 1982.

Winsor, P., Rodhe, J., and Omstedt, A.: Baltic Sea ocean climate: an analysis of 100 yr of hydrographic data with focus on the freshwater budget, Climate Research, 18, 5–15, 2001.

Winton, M.: A reformulated three-layer sea ice model, Journal of atmospheric and oceanic technology, 17, 525–531, 2000.

Zorita, E. and Laine, A.: Dependence of salinity and oxygen concentrations in the Baltic Sea on large-scale atmospheric circulation, Climate Research, 14, 25–41, 2000.